

## Electronic Supplementary Information (ESI)

### **Luminescent terbium(III) probes containing an aromatic amino acid-based antenna for discrimination between adenine and guanine nucleotides**

Sunanda Pradhan, Nitin Shukla,<sup>‡</sup> Goutam Panigrahi<sup>‡</sup> and Ashis K. Patra\*

Department of Chemistry, Indian Institute of Technology Kanpur, Kanpur 208016, Uttar Pradesh, India.

<sup>‡</sup> Authors with equal contribution

E-mail: [akpatra@iitk.ac.in](mailto:akpatra@iitk.ac.in)

## Table of contents

Contents	Page No.
<b>Experimental details and methods</b>	S4
<b>Synthesis and characterization</b>	S7
<b>Fig. S1</b> Synthesis of $L^{aa}$ and $[Tb-L^{aa}]$ complexes ( $L^{aa} = L^{trp}, L^{tyr}, L^{phe}$ ).	S7
<b>Fig. S2</b> Chemical structures of $[Tb-L^{aa}]$ complexes, ( $L^{aa} = L^{trp}, L^{tyr}, L^{phe}$ ).	S13
<b>Fig. S3</b> $^1H$ -NMR (400 MHz) and $^{13}C\{^1H\}$ -NMR (101 MHz) spectrum of <b>S1</b> in $CDCl_3$ at 298 K.	S13
<b>Fig. S4</b> $^1H$ -NMR (400 MHz) and $^{13}C\{^1H\}$ -NMR (101 MHz) spectrum of <b>1a</b> in $D_2O$ at 298 K.	S15
<b>Fig. S5</b> $^1H$ -NMR (400 MHz) and $^{13}C\{^1H\}$ -NMR (101 MHz) spectrum of <b>1b</b> in $D_2O$ at 298 K.	S16
<b>Fig. S6</b> $^1H$ -NMR (400 MHz) and $^{13}C\{^1H\}$ -NMR (101 MHz) spectrum of <b>1c</b> in $D_2O$ at 298 K.	S17
<b>Fig. S7</b> $^1H$ -NMR (400 MHz) and $^{13}C\{^1H\}$ -NMR (101 MHz) spectrum of <b>2a</b> in $CDCl_3$ at 298 K.	S18
<b>Fig. S8</b> $^1H$ -NMR (400 MHz) and $^{13}C\{^1H\}$ -NMR (101 MHz) spectrum of <b>2b</b> in $CDCl_3$ at 298 K.	S19
<b>Fig. S9</b> $^1H$ -NMR (400 MHz) and $^{13}C\{^1H\}$ -NMR (101 MHz) spectrum of <b>2c</b> in $CDCl_3$ at 298 K.	S20
<b>Fig. S10</b> $^1H$ -NMR (400 MHz) and $^{13}C\{^1H\}$ -NMR (101 MHz) spectrum of $L^{trp}$ in $D_2O$ at 298 K.	S21
<b>Fig. S11</b> $^1H$ -NMR (400 MHz) and $^{13}C\{^1H\}$ -NMR (101 MHz) spectrum of $L^{tyr}$ in $D_2O$ at 298 K.	S22
<b>Fig. S12</b> $^1H$ -NMR (400 MHz) and $^{13}C\{^1H\}$ -NMR (101 MHz) spectrum of $L^{phe}$ in $D_2O$ at 298 K.	S23
<b>Fig. S13</b> ESI-MS (+) spectrum (full-range) of $L^{trp}$ in $H_2O$ .	S24
<b>Fig. S14</b> ESI-MS (+) spectrum (full-range) of $L^{tyr}$ in $H_2O$ .	S25
<b>Fig. S15</b> ESI-MS (+) spectrum (full-range) of $L^{phe}$ in $H_2O$ .	S26
<b>Fig. S16</b> The solid-state FT-IR spectrum of (a) $L^{trp}$ , (b) $L^{tyr}$ , and (c) $L^{phe}$ in KBr pellet.	S27

<b>Fig. S17</b> ESI-MS (-) spectrum (full-range) of [Tb-L <sup>trp</sup> ] in H <sub>2</sub> O.	S28
<b>Fig. S18</b> ESI-MS (-) spectrum (full-range) of [Tb-L <sup>tyr</sup> ] in H <sub>2</sub> O.	S28
<b>Fig. S19</b> ESI-MS (-) spectrum (full-range) of [Tb-L <sup>phe</sup> ] in H <sub>2</sub> O.	S29
<b>Fig. S20</b> FT-IR spectrum of (a) [Tb-L <sup>trp</sup> ], (b) [Tb-L <sup>tyr</sup> ], and (c) [Tb-L <sup>phe</sup> ] in KBr pellet.	S30
<b>Fig. S21</b> UV-vis absorption spectrum of (a) L <sup>aa</sup> ligands and (b) [Tb-L <sup>aa</sup> ] complexes (L <sup>aa</sup> = L <sup>trp</sup> , L <sup>tyr</sup> , L <sup>phe</sup> ).	S31
<b>Fig. S22</b> Excitation and emission spectrum of [Tb-L <sup>aa</sup> ] complexes (25 μM), (L <sup>aa</sup> = L <sup>trp</sup> , L <sup>tyr</sup> , L <sup>phe</sup> ).	S31
<b>Fig. S23</b> Fluorescence titration experiments of L <sup>trp</sup> (25 μM) in the presence of different nucleobases, nucleosides, and nucleotides (0.34 mM).	S32
<b>Fig. S24</b> TRL titration experiments of [Tb-L <sup>trp</sup> ] (25 μM) in the presence of different anions (0.64 mM), followed by the addition of GMP (0.64 mM).	S32
<b>Table S1.</b> Luminescence lifetime values in H <sub>2</sub> O/D <sub>2</sub> O and calculated q values of [Tb-L <sup>trp</sup> ].	S33
<b>Fig. S25</b> Luminescence lifetime of [Tb-L <sup>trp</sup> ] in H <sub>2</sub> O/D <sub>2</sub> O, in the absence and presence of 30 eq. purine nucleotides.	S34
<b>Fig. S26</b> TRL titration experiments of [Tb-L <sup>tyr</sup> ] (25 μM) in the presence of different nucleotides (0.44 mM).	S35
<b>Fig. S27</b> TRL titration experiments of [Tb-L <sup>phe</sup> ] (25 μM) in the presence of different nucleotides (0.12 mM).	S35
<b>Fig. S28</b> Stern-Volmer plots and Stern-Volmer quenching constants ( $K_{sv}$ ) of [Tb-L <sup>trp</sup> ] in the presence of different nucleotides.	S36
<b>Fig. S29</b> Plot for the calculation of limit of detection (LOD) for G-NPPs by [Tb-L <sup>trp</sup> ] using TRL-titration data.	S36
<b>Table S2.</b> Calculation of LOD for G-NPPs by [Tb-L <sup>trp</sup> ] using TRL-titration data.	S37
<b>References</b>	S37

---

## **Experimental Details**

**General Considerations.** All the reagent-grade chemicals, HPLC solvents are purchased from commercial suppliers and used without further purification. Dry solvents are prepared using standard procedure. Adenosine tri-phosphate disodium salt (ATP), adenosine di-phosphate sodium salt (ADP), adenosine mono-phosphate hydrate (AMP), guanosine tri-phosphate disodium salt dihydrate (GTP), guanosine di-phosphate disodium salt (GDP), guanosine mono-phosphate disodium salt (GMP) are purchased from Sigma-Aldrich. Silica Gel 100-200 mesh was used for column chromatography purchased from Finer. TLC plates with F254 fluorescent indicator are purchased from Merck. Milli-Q water was used to prepare HEPES buffer solution (10 mM, pH 7.2). All the experiments were carried out at 298 K unless otherwise specified. Plots and graphical representations were done using Origin 9.1 software.

**Instruments.** UV-Vis absorption spectra were recorded using JASCO V-670 spectrophotometer. HEPES buffer (10 mM, pH 7.2) was used as the major solvent for spectroscopic measurements. Perkin Elmer UV/Vis spectroscopic cells made with quartz glass with a 1 cm path length were used throughout the experiments. Absorption spectra were recorded keeping UV-Vis bandwidth 0.2 nm, scan speed 200 nm/min, with 0.5 nm data interval. The Fourier transform infrared spectra (FTIR) were recorded in KBr pellets on a PerkinElmer 1320 instrument in the range 4000 – 400  $\text{cm}^{-1}$ .  $^1\text{H}$ ,  $^{13}\text{C}\{^1\text{H}\}$ -NMR spectra are recorded on a JEOL ECX-400 FT (400 MHz) spectrometer using the deuterated solvents (purchased from Sigma-Aldrich) mentioned in the spectrum and TMS as the internal standard. The chemical shift values and coupling constant values are expressed in ppm and Hz, respectively. The NMR data were processed using MestReNova software. ESI-MS data was obtained using LC-MS (ESI)-QToF (Agilent 6546 LC/Q-TOF) operating in positive and negative modes as stated. Theoretical mass data was obtained from the Molecular weight calculator. The fluorescence and time-resolved luminescence spectra in phosphorescence mode were recorded using Agilent Cary Eclipse fluorescence spectrophotometer. The spectra were recorded using Perkin Elmer Fluorescence cell made with Quartz glass. The emission was recorded in the range of 450 nm to 650 nm using PMT voltage 600 V, with excitation and emission slits of 5 nm. During the experiments, the pH of the solution was measured by Eutech pH-700 pH meter.

**Optical measurements.** The stock solution of 1 mM concentration of three ligands  $\text{L}^{\text{trp}}$ ,  $\text{L}^{\text{tyr}}$ ,  $\text{L}^{\text{phe}}$ , and three Tb(III) complexes:  $[\text{Tb-L}^{\text{trp}}]$ ,  $[\text{Tb-L}^{\text{tyr}}]$ ,  $[\text{Tb-L}^{\text{phe}}]$  were prepared in Milli-Q water. The stock solution of analytes of 5 mM concentration are (except guanosine, guanine,

adenosine, and adenine) prepared in HEPES buffer solution (10 mM, pH 7.2). 1 mM stock solution of guanine, guanosine, adenine and adenosine are prepared in Mili-Q water (pH 8).

UV-vis absorption spectroscopy was performed in HEPES buffer solution (10 mM, pH 7.2) as a major solvent using quartz UV/Vis spectroscopic cells of 1 cm path length. Absorption spectra were recorded keeping UV-Vis bandwidth 0.2 nm, scan speed 200 nm/ min, with 0.5 nm data interval at 298 K. UV-Vis absorption spectra are plotted in Origin 9.1 and molar absorption coefficient values of the ligands and metal complexes are calculated using Beer-Lambert law as follows:

$$A = \epsilon \cdot c \cdot l \dots \dots \dots (1)$$

Here,

$A$  = Absorbance at  $c$  (M) concentration.

$\epsilon$  = Molar absorption coefficient ( $M^{-1}cm^{-1}$ ).

$l$  = Optical path length (cm).

The fluorescence spectrum was measured in HEPES buffer solution (10 mM, pH 7.2) as major solvent using ex./em. slit width of 5 nm. The time-resolved luminescence (TRL) spectra were recorded in medium voltage using delay and gate time of 0.5 ms and ex./em. slit width of 5 nm. The luminescence lifetime of the complexes was measured in H<sub>2</sub>O and D<sub>2</sub>O from the decay of <sup>5</sup>D<sub>4</sub>→<sup>7</sup>F<sub>5</sub> band at 546 nm with a pulsed Xenon arc lamp with a delay and gate time of 0.5 ms. The hydration state ( $q$ ) of Tb(III) complexes is measured using modified Horrocks' equation:

$$q (\text{Tb}) = 5.0 \left( \frac{1}{\tau_{H_2O}} - \frac{1}{\tau_{D_2O}} - 0.06 \right) \dots \dots \dots (2)$$

Here,

$q$  (Tb) = Number of water molecule(s) directly coordinated to the Tb(III) ion.

$\tau_{H_2O}$  = Luminescence lifetime of Tb(III) probe in H<sub>2</sub>O.

$\tau_{D_2O}$  = Luminescence lifetime of Tb(III) probe in D<sub>2</sub>O.

The limit of detection (LOD) of Tb(III) probes were determined from time-resolved luminescence measurements using changes in luminescence intensity for  $^5D_4 \rightarrow ^7F_5$  band at 546 nm, and calculated using the formula as follows:

$$LOD = 3.3 \frac{\sigma}{s} \dots \dots \dots (3)$$

Here,

$\sigma$  = Standard deviation of the regression line.

$s$  = Slope of the linear fraction of the curve at low concentration obtained from the graph of relative luminescence intensity change ( $I/I_0$ ) vs. concentration ( $c$ ) of the analyte.

$I_0$  = Luminescence intensity of Tb(III) probe without addition of analyte.

$I$  = Luminescence intensity of Tb(III) probe after the addition of the analyte.

## Synthesis and characterization of $L^{aa}$ and $[Tb-L^{aa}]$ complexes ( $L^{aa} = L^{trp}, L^{tyr}, L^{phe}$ )

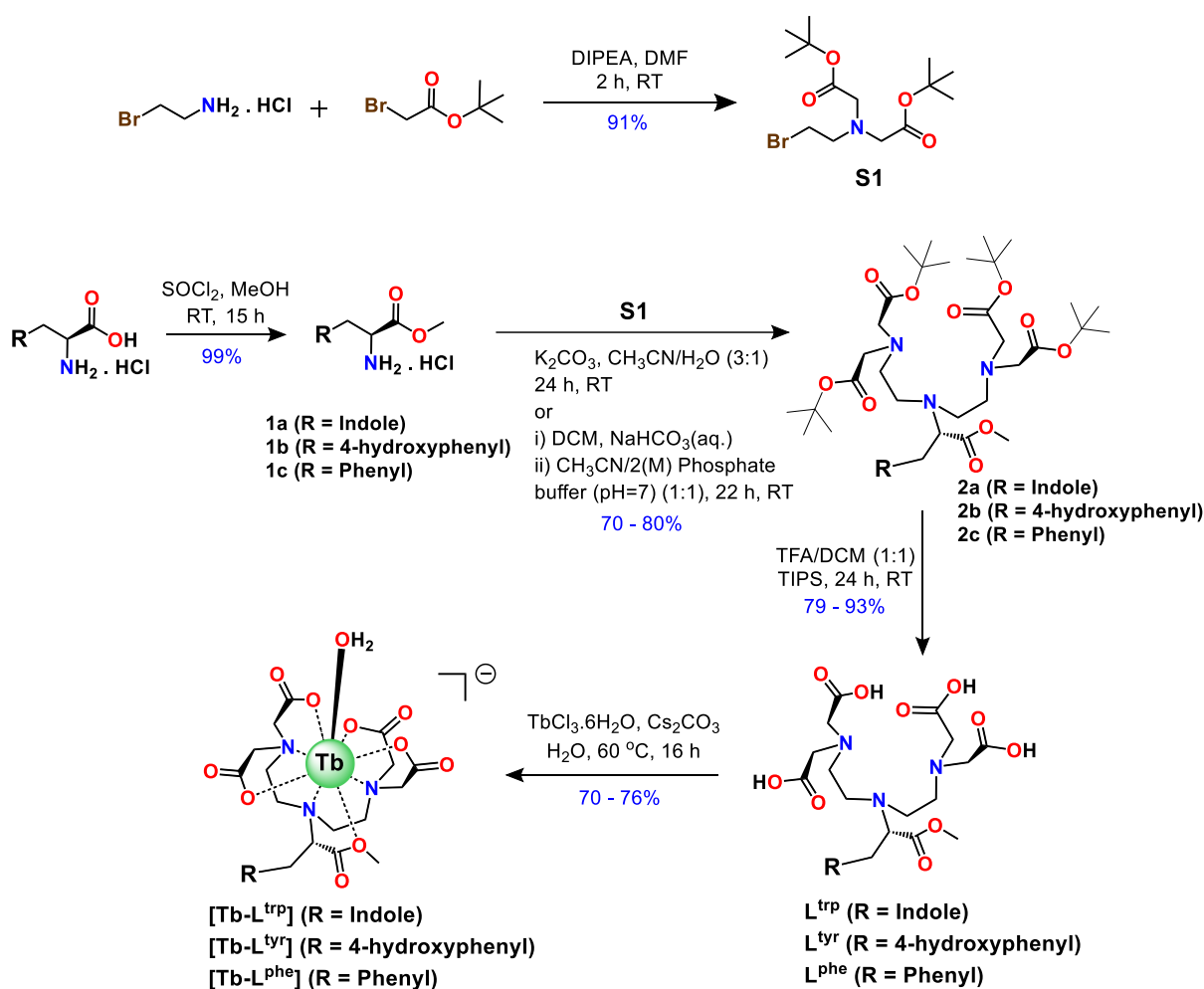


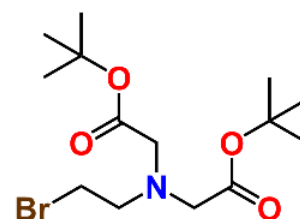
**Fig. S1** Synthetic procedure for the synthesis of  $L^{aa}$  ligands ( $L^{aa} = L^{trp}, L^{tyr}, L^{phe}$ ) and  $[Tb-L^{aa}]$  ( $L^{aa} = L^{trp}, L^{tyr}, L^{phe}$ ) complexes.

### Details of synthesis of $L^{aa}$ ligands ( $L^{aa} = L^{trp}, L^{tyr}, L^{phe}$ )

#### Di-tert-butyl 2,2'-((2-bromoethyl) azanediyl) diacetate ( $S1$ )<sup>1</sup>

In 50 mL R.B., tert-butyl 2-bromoacetate (2.27 mL, 15 mmol) was added in 5 mL of DMF followed by addition of DIPEA (3.5 mL, 20 mmol) and allow to stir for 15 min at RT. A solution of 2-bromoethan-1-amine hydrochloride (1 g, 6 mmol) in 5 mL DMF was added into the stirred reaction mixture and kept stirring for additional 2 h at RT.

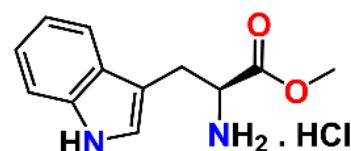
About 400 mL of water was added into this reaction mixture and extracted with 3x100 mL of ethyl acetate. About 20 mL of brine solutions were added each time. The organic portions were collected and anhydrous  $Na_2SO_4$  was added followed by evaporation of solvent and drying under



reduced pressure to yield the light yellow oily crude product. This crude mixture was purified by silica column, elution with 2% ethyl acetate/ hexane mixture afforded the light-yellow oily product (2 g, density = 1.34 gm/mL, yield: 91%).  $^1\text{H}$  NMR (400 MHz,  $\text{CDCl}_3$ )  $\delta$  3.47 (s, 4H), 3.45 – 3.41 (m, 2H), 3.15 – 3.11 (m, 2H), 1.46 (s, 18H).  $^{13}\text{C}$  NMR (101 MHz,  $\text{CDCl}_3$ )  $\delta$  170.56, 81.45, 56.77, 56.58, 30.24, 28.26 (**Fig. S3**).

### Methyl tryptophanate hydrochloride (**1a**)

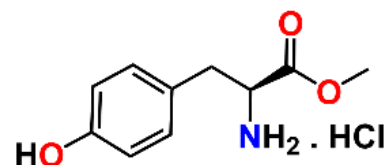
In 100 mL of R.B., 2 g L-tryptophan was taken and 12 mL methanol was added. The mixture was kept under an ice bath for 15 min. About 2 mL of  $\text{SOCl}_2$  was added dropwise carefully into



this ice-cooled mixture. The reaction mixture was allowed to come at RT and it was stirred for 24 h. The clay-type grey compound was formed, and the solvent was evaporated. Methanol was further added and subsequently evaporated. The procedure was repeated 4 times to remove traces of  $\text{SOCl}_2$  and yield a grey color solid (yield: 2.3 g, 99%).  $^1\text{H}$  NMR (400 MHz,  $\text{D}_2\text{O}$ )  $\delta$  7.61 (d,  $J = 8.0$  Hz, 1H), 7.53 (d,  $J = 8.1$  Hz, 1H), 7.33 – 7.22 (m, 2H), 7.22 – 7.16 (m, 1H), 4.50 – 4.42 (m, 1H), 3.80 (s, 3H), 3.55 – 3.42 (m, 2H).  $^{13}\text{C}$  NMR (101 MHz,  $\text{D}_2\text{O}$ )  $\delta$  170.51, 136.33, 126.42, 125.44, 122.30, 119.67, 118.09, 112.12, 106.04, 53.61, 53.36, 25.71 (**Fig. S4**).

### Methyl tyrosinate hydrochloride (**1b**)

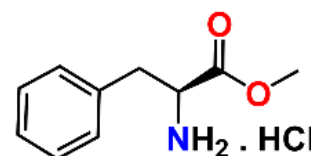
Methyl tyrosinate hydrochloride (**1b**) was synthesized using a similar procedure for **1a**, starting from L-tyrosine (2 g). Yield: 2.35 g, 99%.  $^1\text{H}$  NMR (400 MHz,  $\text{D}_2\text{O}$ )  $\delta$  7.17 (d,  $J = 8.5$  Hz, 2H), 6.91 (d,  $J = 8.5$  Hz, 2H), 4.39 (dd,  $J = 7.3, 5.5$  Hz, 1H),



3.85 (s, 3H), 3.28 (dd,  $J = 14.6, 6.1$  Hz, 1H), 3.18 (dd,  $J = 14.6, 7.3$  Hz, 1H).  $^{13}\text{C}$  NMR (101 MHz,  $\text{D}_2\text{O}$ )  $\delta$  170.17, 155.27, 130.86, 125.43, 116.01, 54.21, 53.54, 34.77 (**Fig. S5**).

### Methyl phenylalaninate hydrochloride (**1c**)

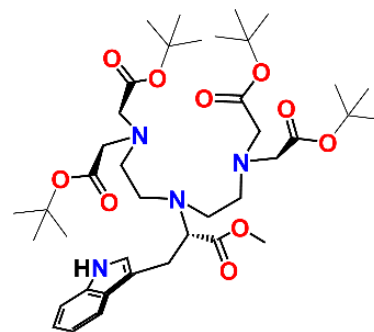
Methyl phenylalaninate hydrochloride (**1c**) was synthesized using a similar procedure as for **1a**, starting from L-phenylalanine. Yield: 2.4 gm, 99%.  $^1\text{H}$  NMR (400 MHz,  $\text{D}_2\text{O}$ )  $\delta$  7.51 – 7.36 (m, 3H), 7.31 (dt,  $J = 5.5, 2.1$  Hz, 2H), 4.45 (dd,  $J = 7.6, 5.8$  Hz, 1H), 3.85 (s,



3H), 3.37 (dd,  $J = 14.3, 5.8$  Hz, 1H), 3.26 (dd,  $J = 14.6, 7.3$  Hz, 1H).  $^{13}\text{C}$  NMR (101 MHz,  $\text{D}_2\text{O}$ )  $\delta$  170.19, 133.86, 129.49, 129.39, 128.23, 54.21, 53.67, 35.69 (**Fig. S6**).

**Tetra-tert-butyl-2,2',2'',2'''-((((3-(1H-indol-3-yl)-1-methoxy-1-oxopropan-2-yl)azanediyl) bis (ethane-2,1-diyl)) bis(azanetriyl)) tetraacetate (2a)**

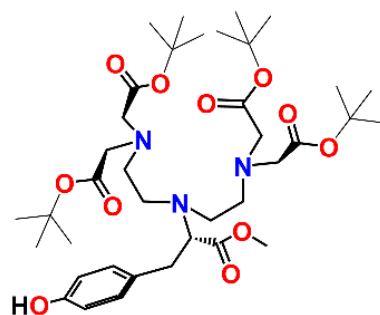
The ligand **2a** was synthesized using a modified literature procedure. In 20 mL acetonitrile: water (3:1) mixture, 500 mg (1.96 mmol) of **1a** and 1.36 g (9.8 mmol) of  $K_2CO_3$  were added and stirred for 10 min at RT. Thereafter, 1.29 mL of **S1** was added dropwise to the stirred solution. The reaction mixture was continuously stirred for 24 h at RT. A greenish-yellow color solution was obtained and the solvent was evaporated under



reduced pressure and extracted 3 times with a DCM-water mixture. The organic phases are collected, anh.  $Na_2SO_4$  was added and the solvent was evaporated under reduced pressure and dried. The light green sticky product was purified by silica column in 40% ethyl acetate/ hexane mixture and afforded a light-yellow sticky product. Yield: 1.14 g, 76%.  $^1H$  NMR (400 MHz,  $CDCl_3$ )  $\delta$  8.08 (s, 1H), 7.60 (d,  $J = 8.0$  Hz, 1H), 7.31 (d,  $J = 8.0$  Hz, 1H), 7.16 (d,  $J = 8.0$  Hz, 1H), 7.13 (d,  $J = 8.0$  Hz, 1H), 7.08 (t,  $J = 7.4$  Hz, 1H), 3.79 – 3.73 (m, 1H), 3.58 (s, 3H), 3.40 (s, 8H), 3.26 (dd,  $J = 14.3, 8.6$  Hz, 1H), 2.99 (dd,  $J = 14.3, 6.3$  Hz, 1H), 2.92 (dt,  $J = 13.2, 7.2$  Hz, 2H), 2.76 (p,  $J = 4.6, 4.0$  Hz, 4H), 2.69 (dd,  $J = 13.2, 5.2$  Hz, 2H), 1.45 (d,  $J = 12.6$  Hz, 36H).  $^{13}C$  NMR (101 MHz,  $CDCl_3$ )  $\delta$  173.14, 170.54, 135.86, 127.44, 123.11, 121.56, 119.06, 118.55, 112.15, 110.82, 80.66, 64.60, 55.84, 53.50, 50.91, 50.34, 27.97, 25.64 (**Fig. S7**).

**Tetra-tert-butyl-2,2',2'',2'''-((((3-(4-hydroxyphenyl)-1-methoxy-1-oxopropan-2-yl)-azane diyl) bis(ethane-2,1-diyl)) bis(azanetriyl)) tetraacetate (2b)**

Ligand **2b** was synthesized from **1b** using the literature procedure for the synthesis of **2a**.<sup>2</sup> At first the acidic compound **1b** (500 mg, 2.16 mmol) was neutralized by saturated  $NaHCO_3$  solution and the neutralized compound was extracted in DCM. The organic portions are collected, anhy.  $Na_2SO_4$  was added to remove the traces of  $H_2O$ , solvent was evaporated and dried

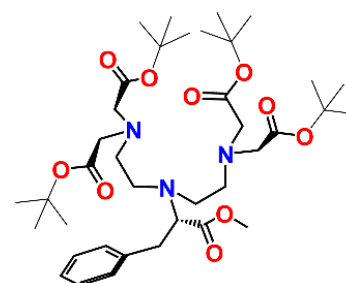


under high vacuum. The white solid thus obtained was dissolved in 20 mL acetonitrile. The ligand **S1** (0.6 mL) and 20 mL of 2(M) phosphate buffer (pH 7) were added and allowed to stir for 3 h at RT. Another portion of **S1** (0.6 mL) was added and stirred for an additional 16 h at the same condition. Again 0.2 ml **S1** was added, and the reaction was stopped after stirring for an additional 3 h. The organic phases were collected and the solvent was evaporated and dried. DCM and water (2:1 v/v) were added to the product, organic parts were collected, and anhy.

Na<sub>2</sub>SO<sub>4</sub> was added, the solvent was evaporated and product was dried. The crude product was purified by silica column (35% ethyl acetate/ hexane) to obtain a white fluffy solid. Yield: 1.1 gm (70%). <sup>1</sup>H NMR (400 MHz, CDCl<sub>3</sub>) δ 7.06 (d, *J* = 8.6 Hz, 2H), 6.70 (d, *J* = 8.6 Hz, 2H), 3.67 – 3.62 (m, 1H), 3.60 (s, 3H), 3.40 (s, 8H), 2.98 (dd, *J* = 13.7, 8.6 Hz, 1H), 2.90 – 2.75 (m, 4H), 2.70 – 2.66 (m, 4H), 2.65 (d, *J* = 5.0 Hz, 1H), 1.45 (s, 36H). <sup>13</sup>C NMR (101 MHz, CDCl<sub>3</sub>) δ 172.95, 170.54, 153.91, 130.41, 130.30, 114.90, 81.19, 80.68, 65.81, 55.93, 53.36, 50.21, 35.16, 28.01 (Fig. S8).

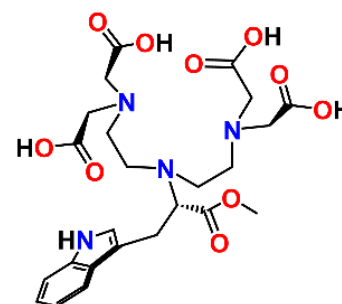
**Tetra-tert-butyl-2,2',2'',2'''-((((1-methoxy-1-oxo-3-phenylpropan-2-yl) azanediyl) bis(ethane-2,1- diyl) bis(azanetriyl)) tetraacetate (2c)**

Ligand **2c** was synthesized from **1c** using a similar procedure used for **2a**. The crude mixture was purified by silica column using 30% ethyl acetate/ hexane mixture that afforded colorless sticky product. Yield: 1.34 gm (80%). <sup>1</sup>H NMR (400 MHz, CDCl<sub>3</sub>) δ 7.24 – 7.18 (m, 4H), 7.16 – 7.12 (m, 1H), 3.71 (t, *J* = 7.4 Hz, 1H), 3.59 (s, 3H), 3.37 (s, 8H), 3.08 – 3.02 (m, 1H), 2.89 – 2.77 (m, 3H), 2.67 (qd, *J* = 5.2, 2.3 Hz, 5H), 2.64 – 2.62 (m, 1H), 1.44 (s, 36H). <sup>13</sup>C NMR (101 MHz, CDCl<sub>3</sub>) δ 173.13, 170.74, 138.76, 129.52, 128.20, 126.23, 80.88, 65.86, 56.18, 53.61, 51.18, 50.48, 36.46, 28.26 (Fig. S9).



**2,2',2'',2'''-((((3-(1H-indol-3-yl)-1-methoxy-1-oxopropan-2-yl) azanediyl) bis(ethane-2,1- (azanetriyl)) tetraacetic acid (L<sup>trp</sup>)**

The pentaester **2a** (100 mg, 0.131 mmol, 1 equiv.) dissolved in 2 mL DCM was stirred in ice bath for 15 min. Triisopropylsilane (134.6 μL, 0.657 mmol, 5 equiv.) was added to this cold reaction mixture. Trifluoroacetic acid (TFA) (2 mL) was added dropwise into this ice-cold solution. The reaction was allowed to reach RT and continued to stir for 24 h. The excess TFA was removed by

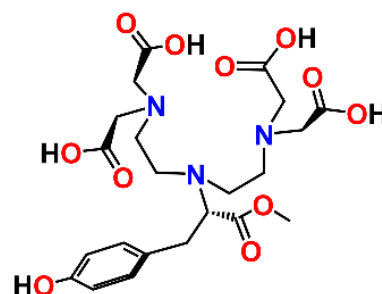


N<sub>2</sub> bubbling and the solvent was removed under reduced pressure. Into this dark brown solution, Et<sub>2</sub>O was added and the precipitate was collected by filtration. The light grey color solid was washed five times with Et<sub>2</sub>O and acetone to yield a white hygroscopic product, which was stored in a desiccator over anh. CaCl<sub>2</sub>. Yield: 56.13 mg, 79.6%. <sup>1</sup>H NMR (400 MHz, D<sub>2</sub>O) δ 7.70 (d, *J* = 7.6 Hz, 1H), 7.51 (d, *J* = 7.9 Hz, 1H), 7.25 (d, *J* = 7.0 Hz, 2H), 7.20 (t, *J* = 6.8

Hz, 1H), 4.08 – 4.00 (m, 1H), 3.91 (s, 8H), 3.68 (s, 3H), 3.42 – 3.36 (m, 1H), 3.33 (dd,  $J = 9.8$ , 4.4 Hz, 4H), 3.21 (dd,  $J = 15.0$ , 8.3 Hz, 1H), 3.09 (tt,  $J = 14.5$ , 7.3 Hz, 4H).  $^{13}\text{C}$  NMR (101 MHz,  $\text{D}_2\text{O}$ )  $\delta$  174.49, 168.87, 136.22, 126.32, 124.43, 122.27, 119.57, 118.25, 112.22, 109.84, 62.96, 55.60, 53.42, 52.50, 45.54, 24.21 (**Fig. S10**). FT-IR ( $\text{cm}^{-1}$ , KBr pallet): 3407 ( $\nu_{\text{O-H}}$ ), 3017 ( $\nu_{\text{Csp}^2\text{-H}}$ ), 1732 ( $\nu_{\text{C=O}}$ ), 1208 ( $\nu_{\text{C-O}}$ ) (**Fig. S16(a)**). ESI-MS (+) in  $\text{H}_2\text{O}$ :  $m/z$   $[\text{M}+\text{H}]^+$  exp.: 537.2185, calcd.: 537.2192 (**Fig. S13**). UV-vis (10 mM HEPES, pH 7.2):  $\lambda_{\text{max}}$  ( $\epsilon/\text{Lmol}^{-1}\text{cm}^{-1}$ ) = 282 nm (4478), 288 nm (4170) (**Fig. S21(a)**).

**2,2',2'',2'''-((((3-(4-hydroxyphenyl)-1-methoxy-1-oxopropan-2-yl) azanediyl) bis(ethane-2,1-diyl)) bis(azanetriyl)) tetraacetic acid ( $\text{L}^{\text{tyr}}$ )**

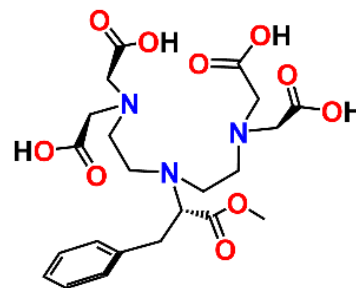
Pentaester **2b** (100 mg, 0.135 mmol, 1 equiv.) was dissolved in 2 mL DCM and stirred in an ice bath for 15 min. Triisopropylsilane (138.8  $\mu\text{L}$ , 0.678 mmol, 5 equiv.) was added to this cold reaction mixture. Trifluoroacetic acid (TFA) (2 mL) was added dropwise into this ice-cold solution. The reaction was allowed to reach RT and stirred for 24 h.



Excess TFA was removed by  $\text{N}_2$  bubbling and the compound was dried under reduced pressure.  $\text{Et}_2\text{O}$  was added to this dark brown solution and the precipitate was collected by filtration, washed two times with  $\text{Et}_2\text{O}$  to yield a white hygroscopic product, stored in a desiccator over anhy.  $\text{CaCl}_2$ . Yield: 63 mg (90%).  $^1\text{H}$  NMR (400 MHz,  $\text{D}_2\text{O}$ )  $\delta$  7.14 (d,  $J = 11.8$  Hz, 2H), 6.82 (d,  $J = 8.6$  Hz, 2H), 3.98 (s, 8H), 3.75 (t,  $J = 7.7$  Hz, 1H), 3.62 (s, 3H), 3.56 – 3.43 (m, 1H), 3.38 (s, 4H), 3.07 (t,  $J = 6.8$  Hz, 4H), 2.90 (dd,  $J = 13.8$ , 7.0 Hz, 1H).  $^{13}\text{C}$  NMR (101 MHz,  $\text{D}_2\text{O}$ )  $\delta$  174.13, 169.12, 154.49, 130.59, 129.20, 115.74, 64.71, 56.06, 53.38, 52.44, 45.69, 33.38 (**Fig. S11**). FT-IR (KBr pallet): 3423  $\text{cm}^{-1}$  ( $\nu_{\text{O-H}}$  of ArO-H), 3265  $\text{cm}^{-1}$  ( $\nu_{\text{O-H}}$  of C(O)O-H), 3020  $\text{cm}^{-1}$  ( $\nu_{\text{Csp}^2\text{-H}}$ ), 1731  $\text{cm}^{-1}$  ( $\nu_{\text{C=O}}$ ), 1240  $\text{cm}^{-1}$  ( $\nu_{\text{C-O}}$ ) (**Fig. S16(b)**). ESI-MS (+) in  $\text{H}_2\text{O}$ :  $m/z$   $[\text{M}+\text{H}]^+$  exp.: 514.2035, calcd.: 514.2032 (**Fig. S14**). UV-vis (10 mM HEPES, pH 7.2):  $\lambda_{\text{max}}$  ( $\epsilon/\text{Lmol}^{-1}\text{cm}^{-1}$ ) = 275 nm (2529) (**Fig. S21(a)**).

**2,2',2'',2'''-((((1-methoxy-1-oxo-3-phenylpropan-2-yl) azanediyl) bis(ethane-2,1-diyl)) bis(azanetriyl)) tetraacetic acid ( $\text{L}^{\text{phe}}$ )**

Ligand  $L^{\text{phe}}$  was synthesized from **2c** (100 mg, 0.2 mmol, 1 equiv.) and purified by a similar procedure as used for  $L^{\text{tyr}}$  obtained as white hygroscopic product which was stored in a desiccator over anhy.  $\text{CaCl}_2$ . Yield: 64 mg (93%).  $^1\text{H}$  NMR (400 MHz,  $\text{D}_2\text{O}$ )  $\delta$  7.36 (t,  $J = 7.5$  Hz, 2H), 7.29 (d,  $J = 3.6$  Hz, 3H), 4.03 (s, 8H), 3.83 (t,  $J = 7.5$  Hz, 1H), 3.63 (s, 3H), 3.52 (dt,  $J = 7.1, 5.8$  Hz, 1H), 3.39 (t,  $J = 7.5$  Hz, 4H), 3.09 (d,  $J = 6.8$  Hz, 4H), 3.01 (dd,  $J = 13.6, 7.2$  Hz, 1H).  $^{13}\text{C}$  NMR (101 MHz,  $\text{D}_2\text{O}$ )  $\delta$  174.13, 168.92, 137.57, 129.26, 129.06, 127.20, 64.64, 55.85, 53.49, 52.49, 45.72, 34.21 (**Fig. S12**). FT-IR ( $\text{cm}^{-1}$ , KBr pallet): 3433 ( $\nu_{\text{O-H}}$ ), 3026 ( $\nu_{\text{Csp}^2\text{-H}}$ ), 1735 ( $\nu_{\text{C=O}}$ ), 1196 ( $\nu_{\text{C-O}}$ ) (**Fig. S16(c)**). ESI-HRMS (+) in  $\text{H}_2\text{O}$ :  $m/z$   $[\text{M}+\text{H}]^+$  exp.: 498.2089, calcd.: 498.2083. (**Fig. S15**). UV-vis (10 mM HEPES, pH 7.2):  $\lambda_{\text{max}}$  ( $\epsilon/\text{Lmol}^{-1}\text{cm}^{-1}$ ) = 258 nm (918) (**Fig. S21(a)**).



**General procedure for the synthesis of terbium(III) complexes ( $\text{Cs}[\text{Tb-L}^{\text{aa}}]$ ) ( $L^{\text{aa}} = L^{\text{trp}}, L^{\text{tyr}}, L^{\text{phe}}$ ):**

The respective tetraacetic acids ( $L^{\text{aa}}$ ) (0.1 mmol) were dissolved in 2 mL of Mili-Q water. The pH of the ligand solution was adjusted between 7-8 by adding a saturated aqueous solution of  $\text{Cs}_2\text{CO}_3$ . Then, 1 mL of  $\text{TbCl}_3 \cdot 6\text{H}_2\text{O}$  (0.1 mmol) solution in Mili-Q water was added dropwise into the deprotonated ligand solution and stirred at  $60^\circ\text{C}$  for 16 h. The reaction mixture was filtered, and the solvent was dried under vacuum, the product was dried three times with DCM under reduced pressure to yield the desired  $\text{Cs}[\text{Tb-L}^{\text{aa}}]$  complexes in good yields. The respective complexes were characterized by FT-IR and ESI-MS techniques.

The presence of a minor trace of t-butylated side product was observed in the ESI-MS of the  $L^{\text{aa}}$  ligands, however, we did not observe any major  $m/z$  peaks in the ESI-MS analysis of the  $[\text{Tb-L}^{\text{aa}}]$  luminescent probes.

#### **$[\text{Tb-L}^{\text{trp}}]$**

Light grey hygroscopic product. Yield: 57.93 mg, 70.28%. FT-IR ( $\text{cm}^{-1}$ / KBr pallet): 3253 ( $\nu_{\text{O-H}}$ ), 2968 ( $\nu_{\text{Csp}^2\text{-H}}$ ), 1577 ( $\nu_{\text{C=O}}$ ), 1200 ( $\nu_{\text{C-O}}$ ) (**Fig. S20(a)**). ESI-MS (-) in  $\text{H}_2\text{O}$ :  $m/z$   $[\text{M}]^-$  exp.: 691.1041, calcd.: 691.1059, the observed isotopic distribution matched with the calculated one (**Fig. S17**). UV-vis (10 mM HEPES, pH 7.2):  $\lambda_{\text{max}}$  ( $\epsilon/\text{Lmol}^{-1}\text{cm}^{-1}$ ) = 286 nm (3000), 292 nm (2843) (**Fig. S21(b)**).

### [Tb-L<sup>tyr</sup>]

White hygroscopic product. Yield: 58.16 mg, 72.58%. FT-IR (cm<sup>-1</sup>/KBr pallet): 3233 ( $\nu_{\text{O-H}}$ ), 3026 ( $\nu_{\text{Csp}^2\text{-H}}$ ), 1574 ( $\nu_{\text{C=O}}$ ), 1195 ( $\nu_{\text{C-O}}$ ) (**Fig. S20(b)**). ESI-MS (-) in H<sub>2</sub>O:  $m/z$  [M]<sup>-</sup> exp.: 668.0896, calcd.: 668.0899, the observed isotopic distribution matched with the calculated one (**Fig. S18**). UV-vis (10 mM HEPES, pH 7.2):  $\lambda_{\text{max}}$  ( $\epsilon/\text{Lmol}^{-1}\text{cm}^{-1}$ ) = 276 nm (1303) (**Fig. S21(b)**).

### [Tb-L<sup>phe</sup>]

White hygroscopic product. Yield: 58.9 mg, 76.4%. FT-IR (cm<sup>-1</sup>/KBr pallet): 3220 ( $\nu_{\text{O-H}}$ ), 3026 ( $\nu_{\text{Csp}^2\text{-H}}$ ), 1578 ( $\nu_{\text{C=O}}$ ), 1200 ( $\nu_{\text{C-O}}$ ) (**Fig. S20(c)**). ESI-MS (-) in H<sub>2</sub>O:  $m/z$  [M]<sup>-</sup> exp.: 652.0968, calcd.: 652.0950, the observed isotopic distribution matched with the calculated one (**Fig. S19**). UV-vis (10 mM HEPES, pH 7.2):  $\lambda_{\text{max}}$  ( $\epsilon/\text{Lmol}^{-1}\text{cm}^{-1}$ ) = 259 nm (744) (**Fig. S21(b)**).

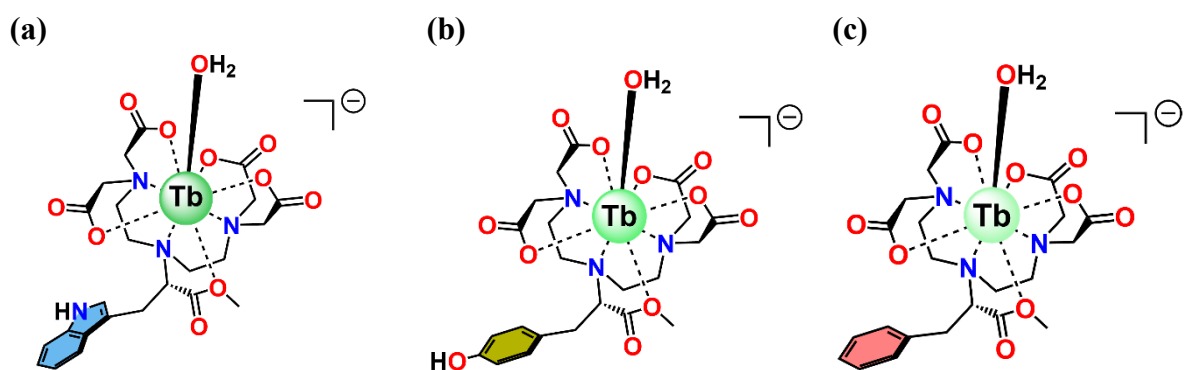


**Fig. S2** The chemical structures of the Tb(III) complexes (a) [Tb-L<sup>trp</sup>], (b) [Tb-L<sup>tyr</sup>], (c) [Tb-L<sup>phe</sup>] with Cs<sup>+</sup> as counter cation studied in this work. The eight-coordinated DTTA moiety strongly chelates with the Tb(III) center. One H<sub>2</sub>O molecule bound with the Tb(III) center (hydration no.,  $q = 1$ ) was confirmed by the spectroscopic experiments.

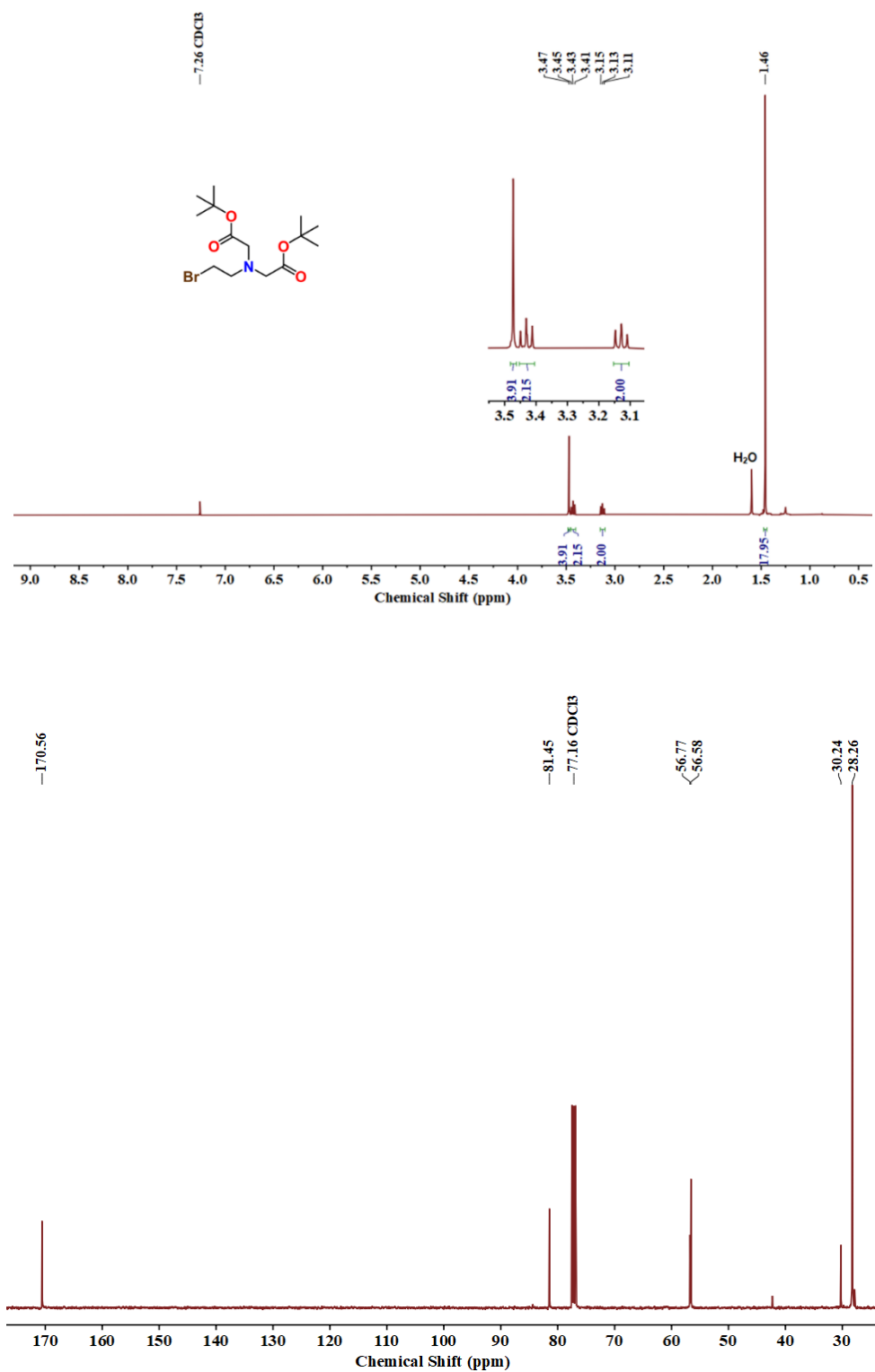


**Fig. S3** <sup>1</sup>H-NMR (400 MHz) (*top*) and <sup>13</sup>C{<sup>1</sup>H}-NMR (101 MHz) spectrum (*bottom*) of S1 in CDCl<sub>3</sub> recorded at 298 K.

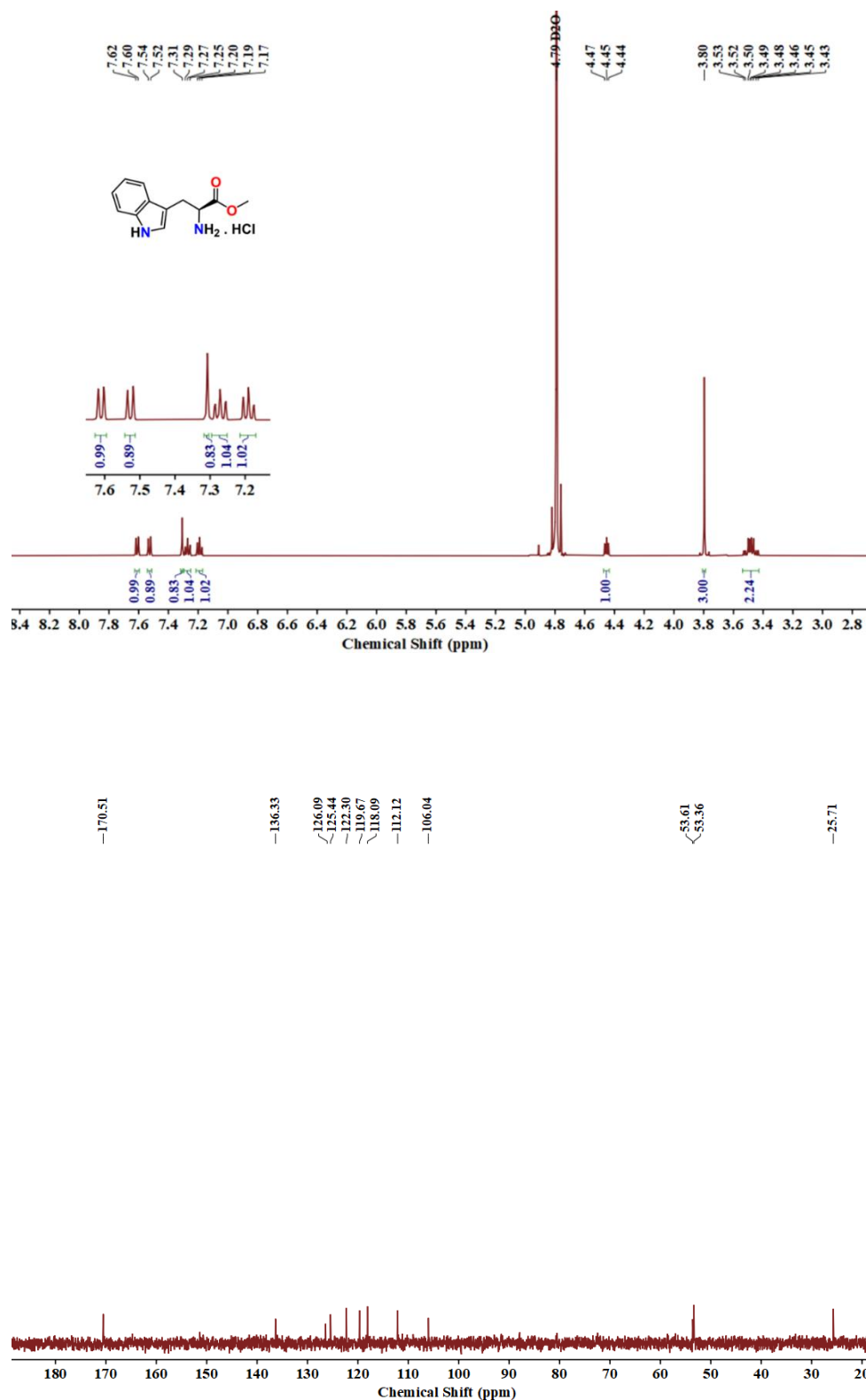


**Fig. S4** <sup>1</sup>H-NMR (400 MHz) (*top*) and <sup>13</sup>C{<sup>1</sup>H}-NMR (101 MHz) spectrum (*bottom*) of **1a** in D<sub>2</sub>O recorded at 298 K.

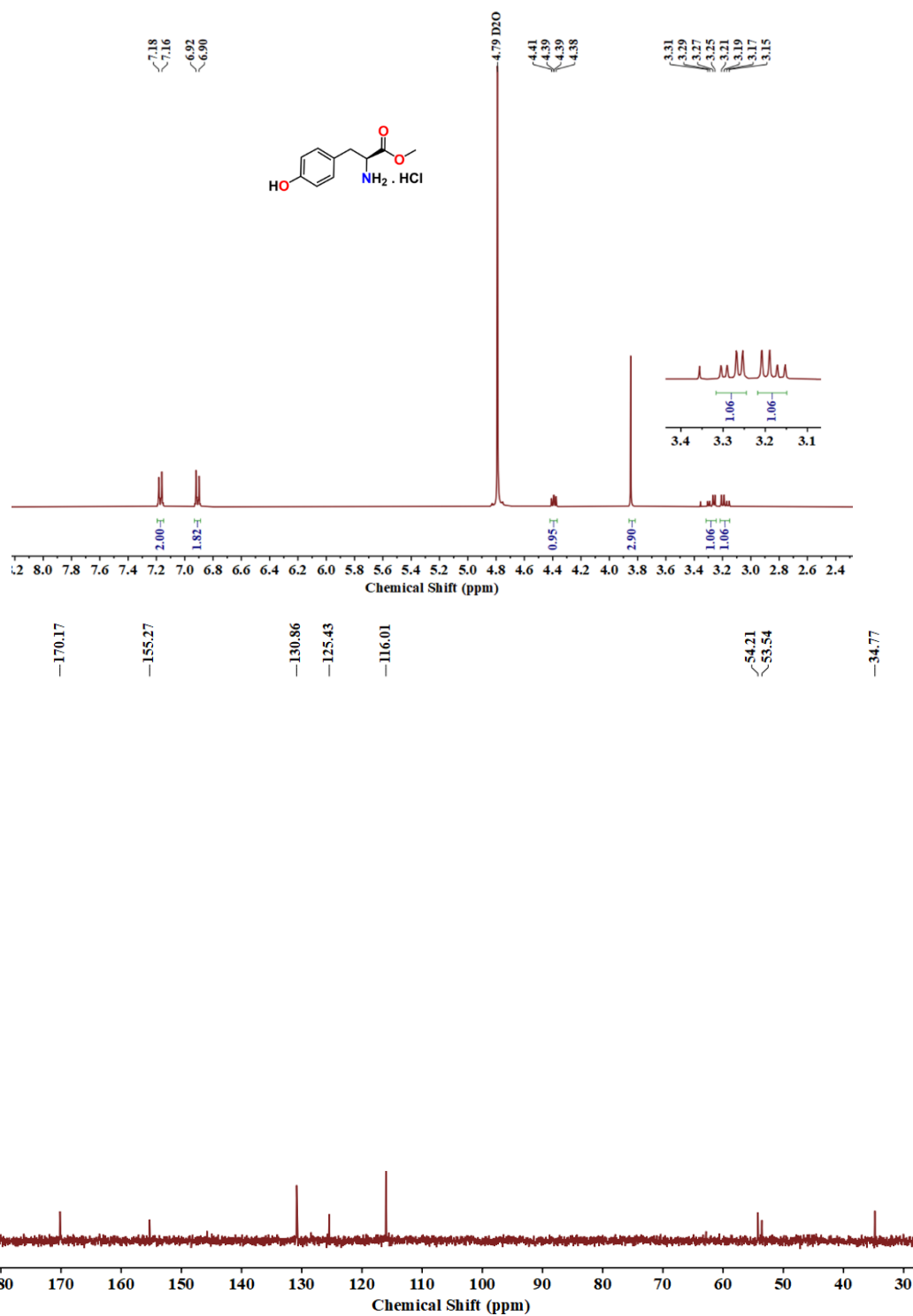


**Fig. S5** <sup>1</sup>H-NMR (400 MHz) (*top*) and <sup>13</sup>C{<sup>1</sup>H}-NMR (101 MHz) spectrum (*bottom*) of **1b** in D<sub>2</sub>O recorded at 298 K.

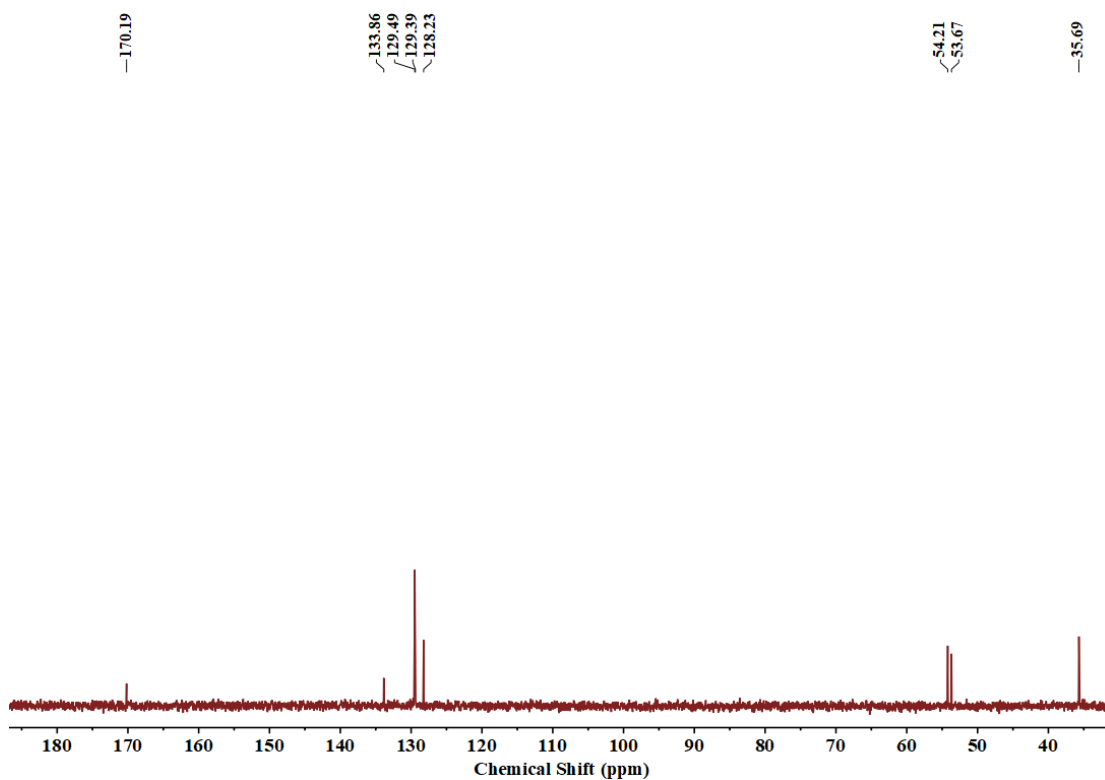
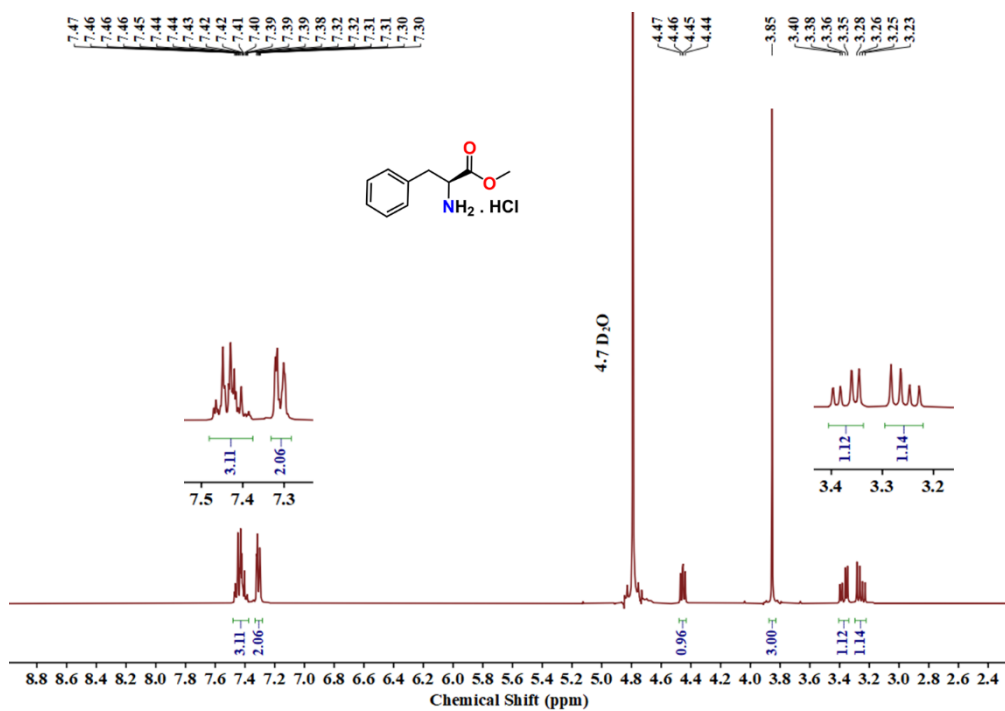


**Fig. S6** <sup>1</sup>H-NMR (400 MHz) (*top*) and <sup>13</sup>C{<sup>1</sup>H}-NMR (101 MHz) spectrum (*bottom*) of **1c** in D<sub>2</sub>O recorded at 298 K.





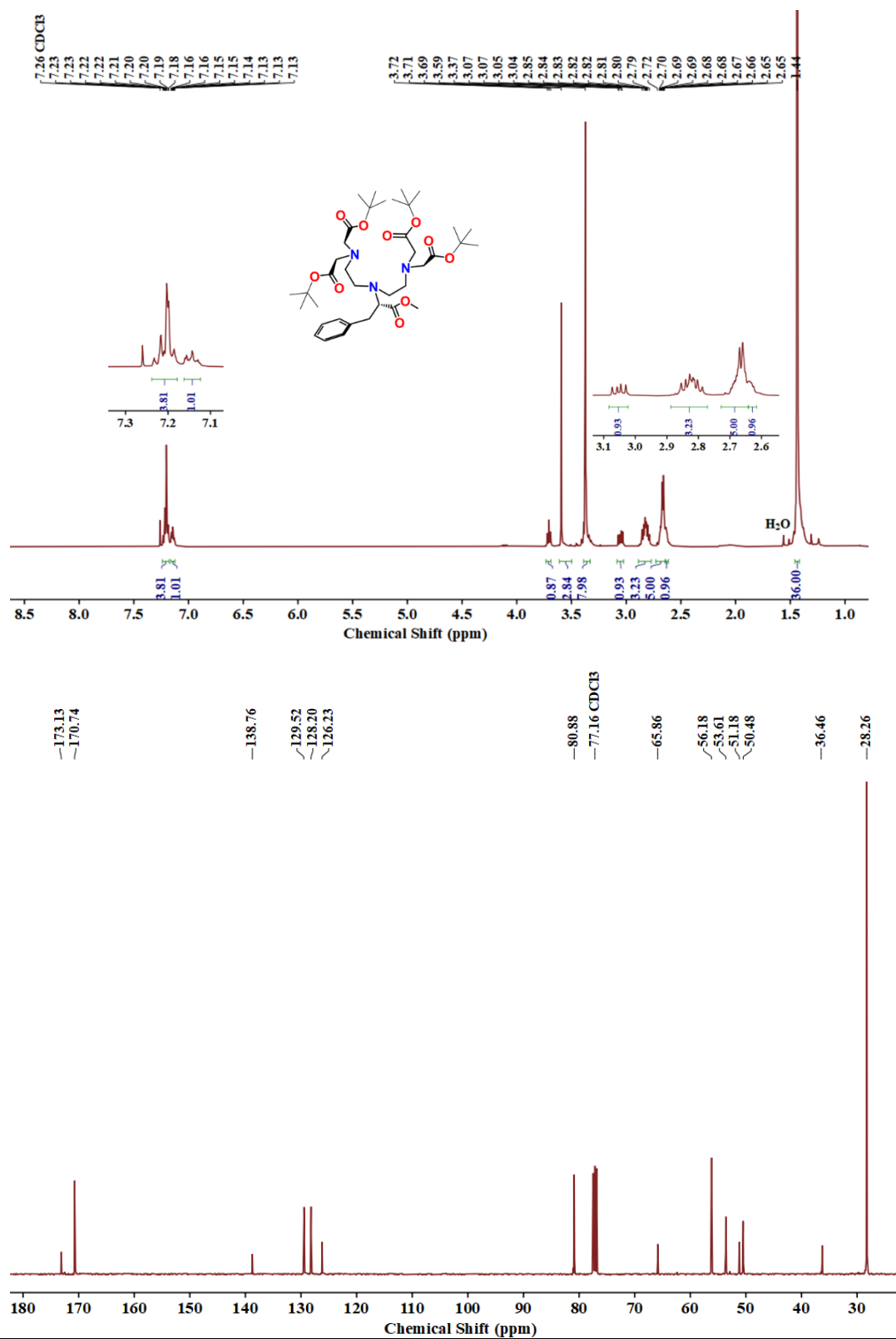


**Fig. S9**  $^1\text{H}$ -NMR (400 MHz) (*top*) and  $^{13}\text{C}\{^1\text{H}\}$ -NMR (101 MHz) spectrum (*bottom*) of **2c** in  $\text{CDCl}_3$  recorded at 298 K.

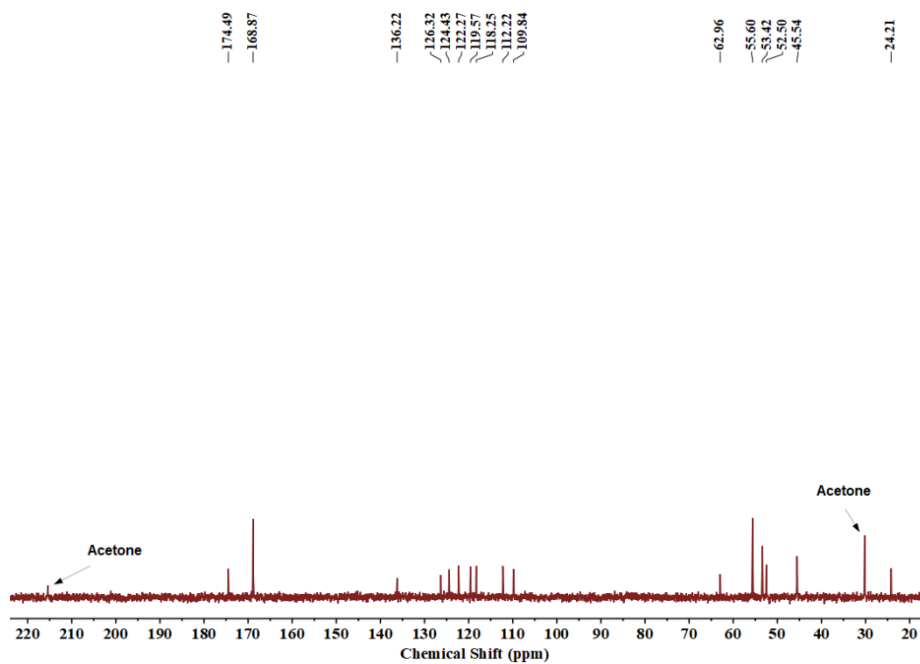
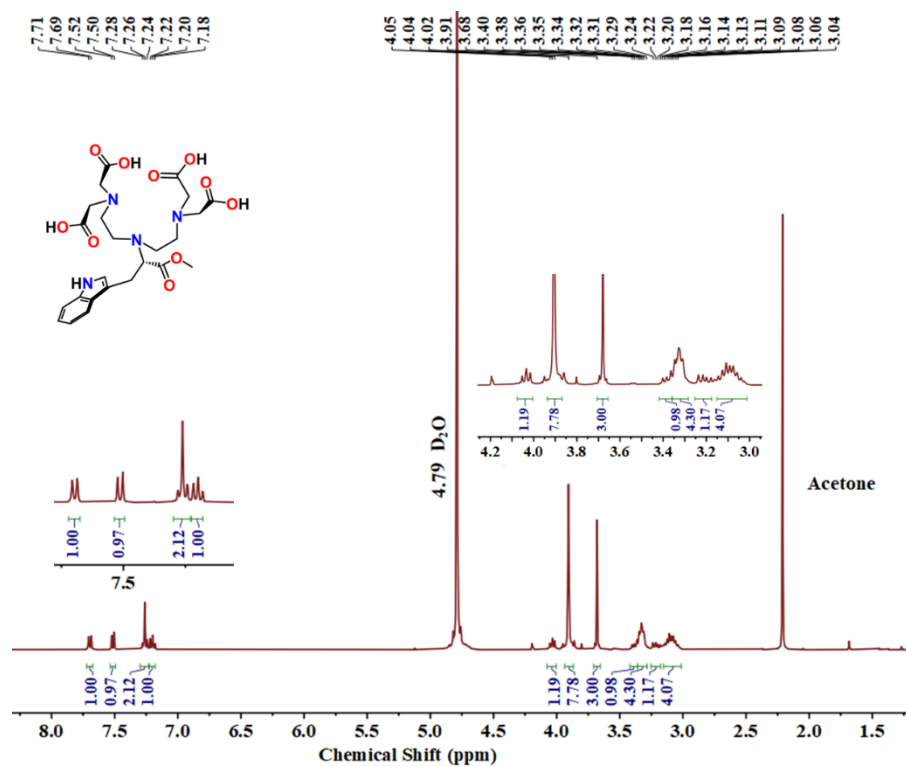


**Fig. S10**  $^1\text{H}$ -NMR (400 MHz) (*top*) and  $^{13}\text{C}\{^1\text{H}\}$ -NMR (101 MHz) spectrum (*bottom*) of  $L^{trp}$  in  $\text{D}_2\text{O}$  recorded at 298 K.

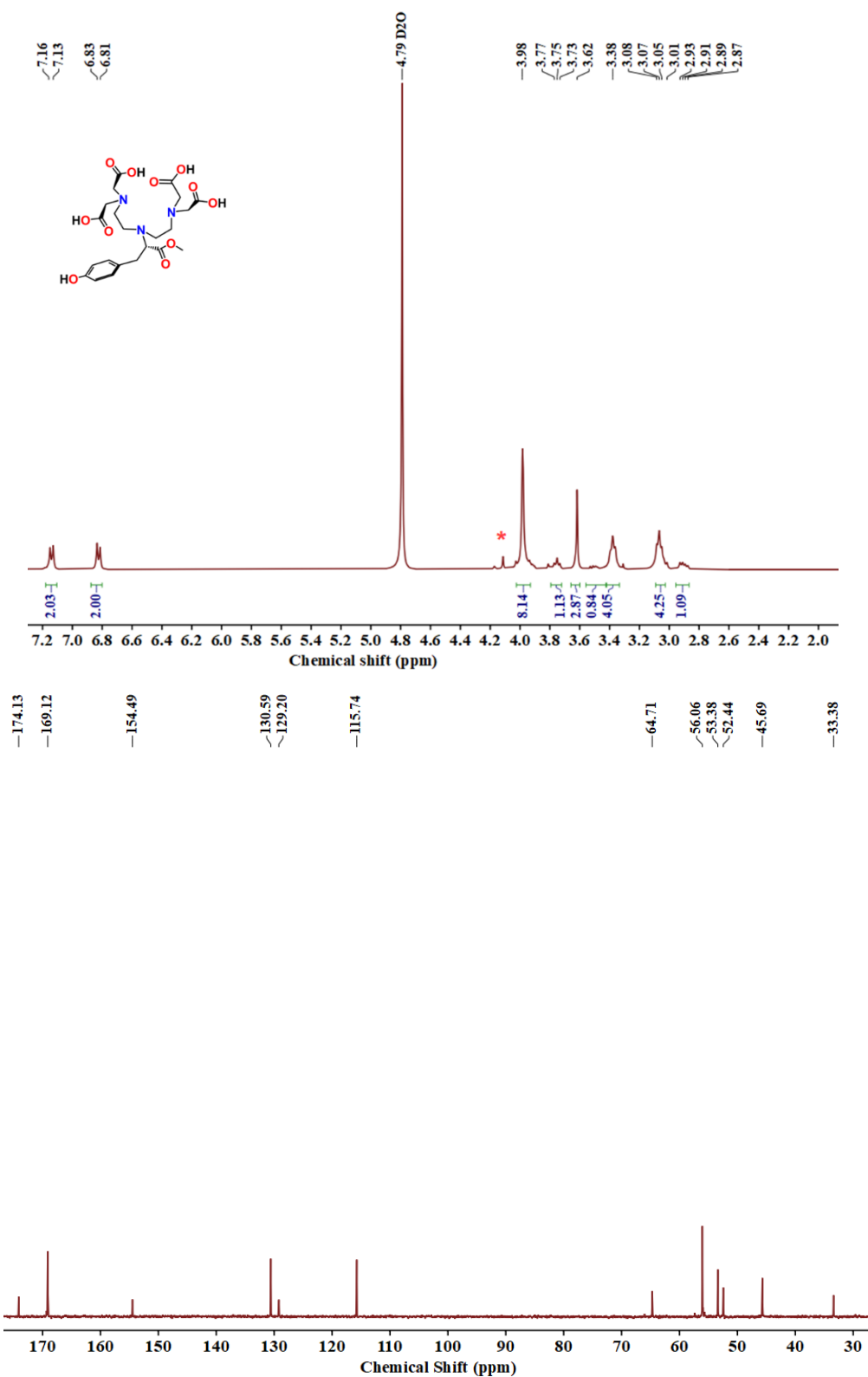


**Fig. S11**  $^1H$ -NMR (400 MHz) (*top*) and  $^{13}C\{^1H\}$ -NMR (101 MHz) spectrum (*bottom*) of  $L^{tyr}$  in  $D_2O$  recorded at 298 K. Unidentified peak is denoted by asterisk (\*) mark.

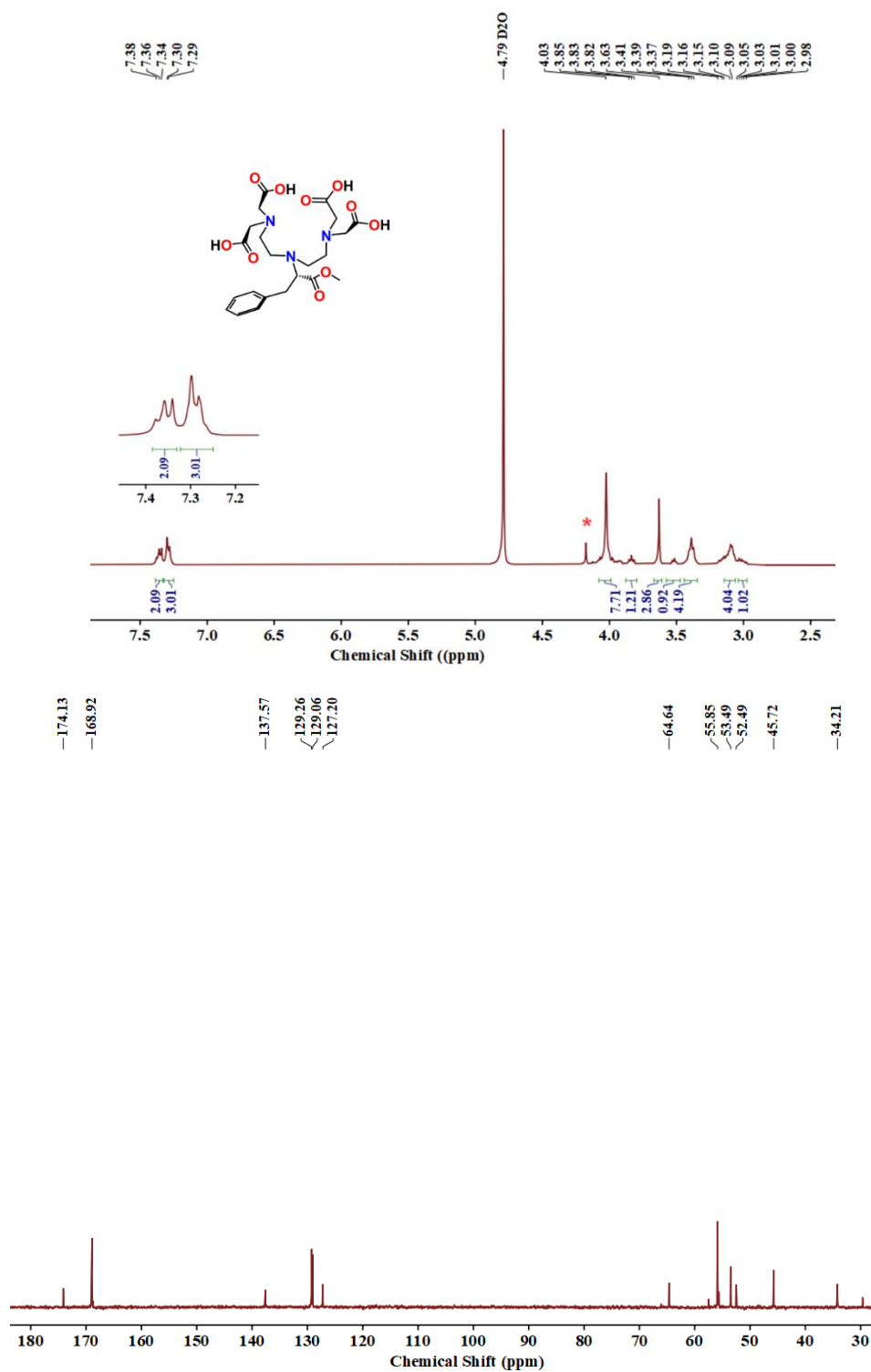


**Fig. S12**  $^1\text{H-NMR}$  (400 MHz) (*top*) and  $^{13}\text{C}\{^1\text{H}\}$ -NMR (101 MHz) spectrum (*bottom*) of  $L^{\text{phe}}$  in  $\text{D}_2\text{O}$  recorded at 298 K. Unidentified peak is denoted by asterisk (\*) mark.

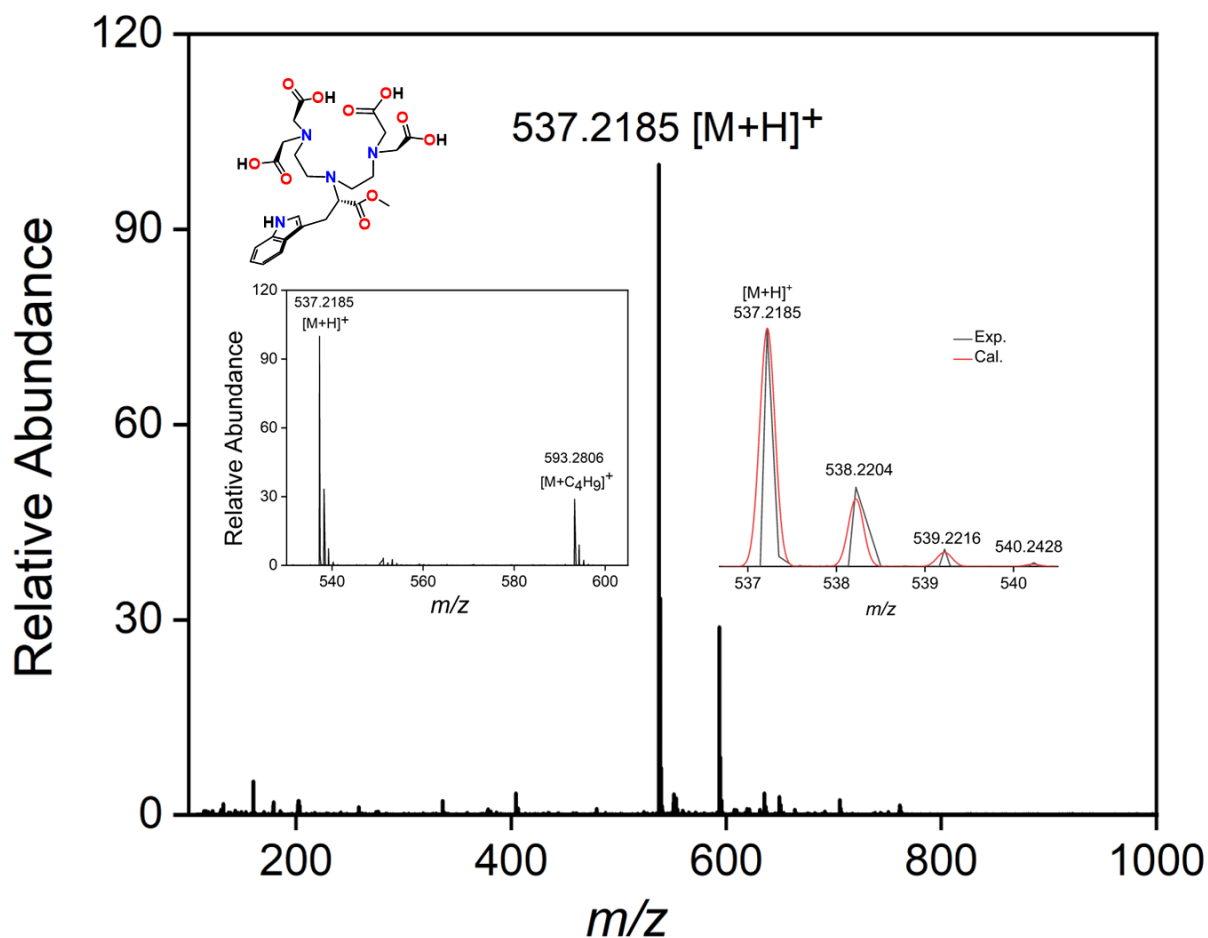


**Fig. S13** ESI-MS (+) spectra (full range) of  $L^{trp}$  in  $H_2O$ . Overlay of experimental isotopic distribution profile with theoretically calculated  $m/z$  value of molecular ion peak (*right inset*).  $m/z$  for  $[M+H]^+$ : exp.: 537.2185, calcd.: 537.2192. Expanded spectrum (*left inset*) showing the presence of a trace of *t*-butylated product peak at  $m/z$  593.2806 for  $[M+C_4H_9]^+$ .

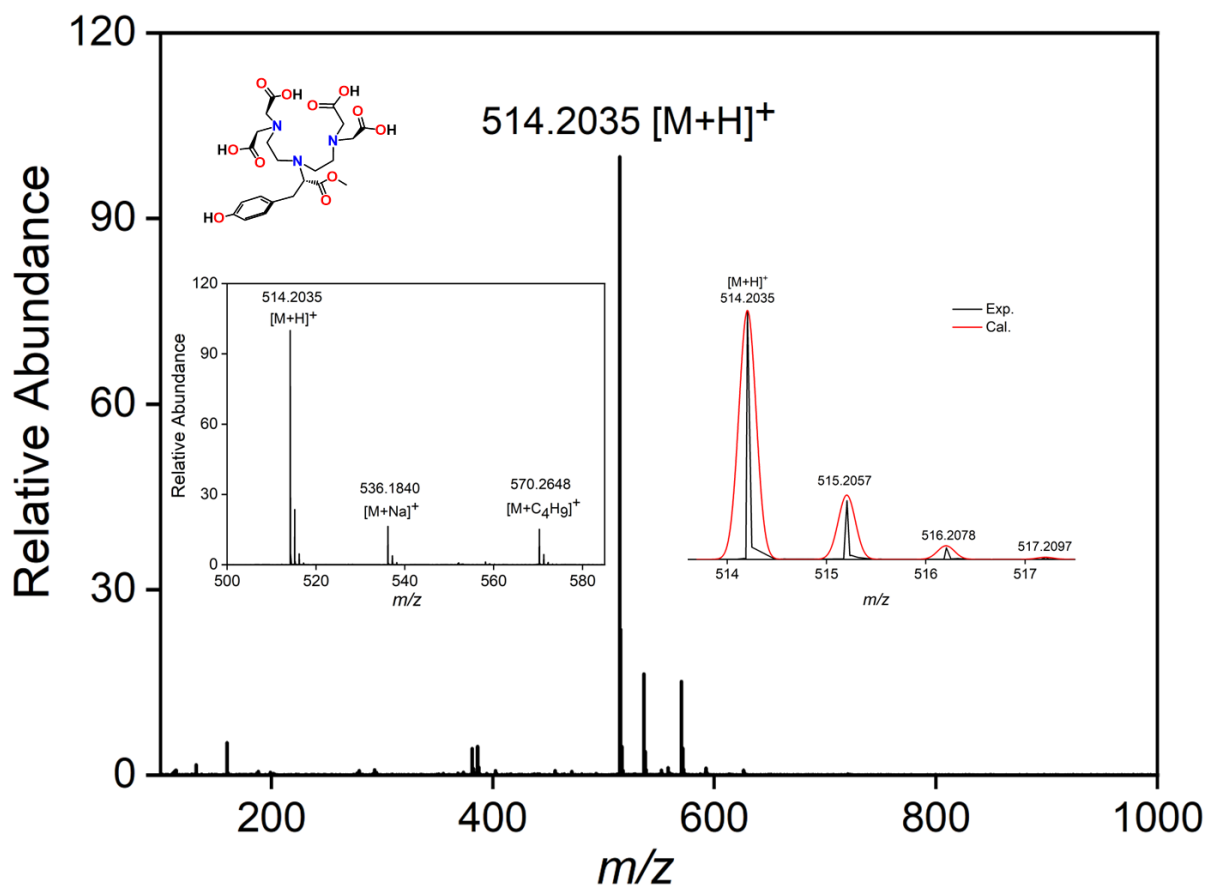


**Fig. S14** ESI-MS (+) spectra (full range) of  $L^{\text{tyr}}$  in  $\text{H}_2\text{O}$ . Overlay of experimental isotopic distribution profile with theoretically calculated  $m/z$  value of molecular ion peak (*right inset*).  $m/z$  for  $[\text{M}+\text{H}]^+$ : exp.: 514.2035, calcd.: 514.2032. Expanded spectrum (*left inset*) showing the presence of  $[\text{M}+\text{Na}]^+$  at  $m/z$  536.1840, and a trace of *t*-butylated product peak at 570.2648 for  $[\text{M}+\text{C}_4\text{H}_9]^+$ , respectively.

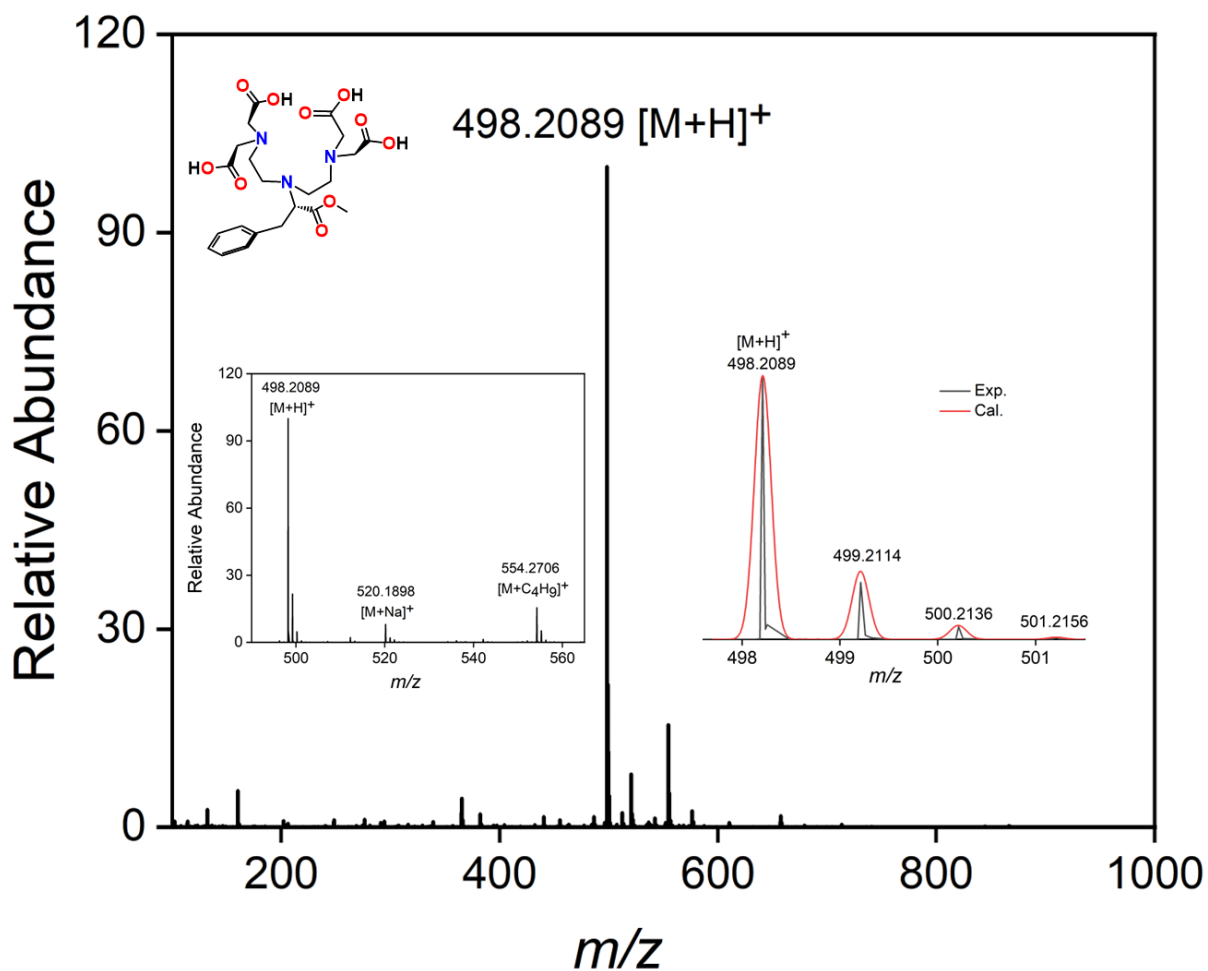


**Fig. S15.** ESI-MS (+) spectra (full range) of L<sup>phe</sup> in H<sub>2</sub>O. Overlay of experimental isotopic distribution profile with theoretically calculated *m/z* value of molecular ion peak (*right inset*). *m/z* for [M+H]<sup>+</sup>: exp.: 498.2089, calcd.: 498.2083. Expanded spectrum (*left inset*) showing the presence of [M+Na]<sup>+</sup> at *m/z* 520.1898, and a trace *t*-butylated product peak at 554.2706 for [M+C<sub>4</sub>H<sub>9</sub>]<sup>+</sup>, respectively.

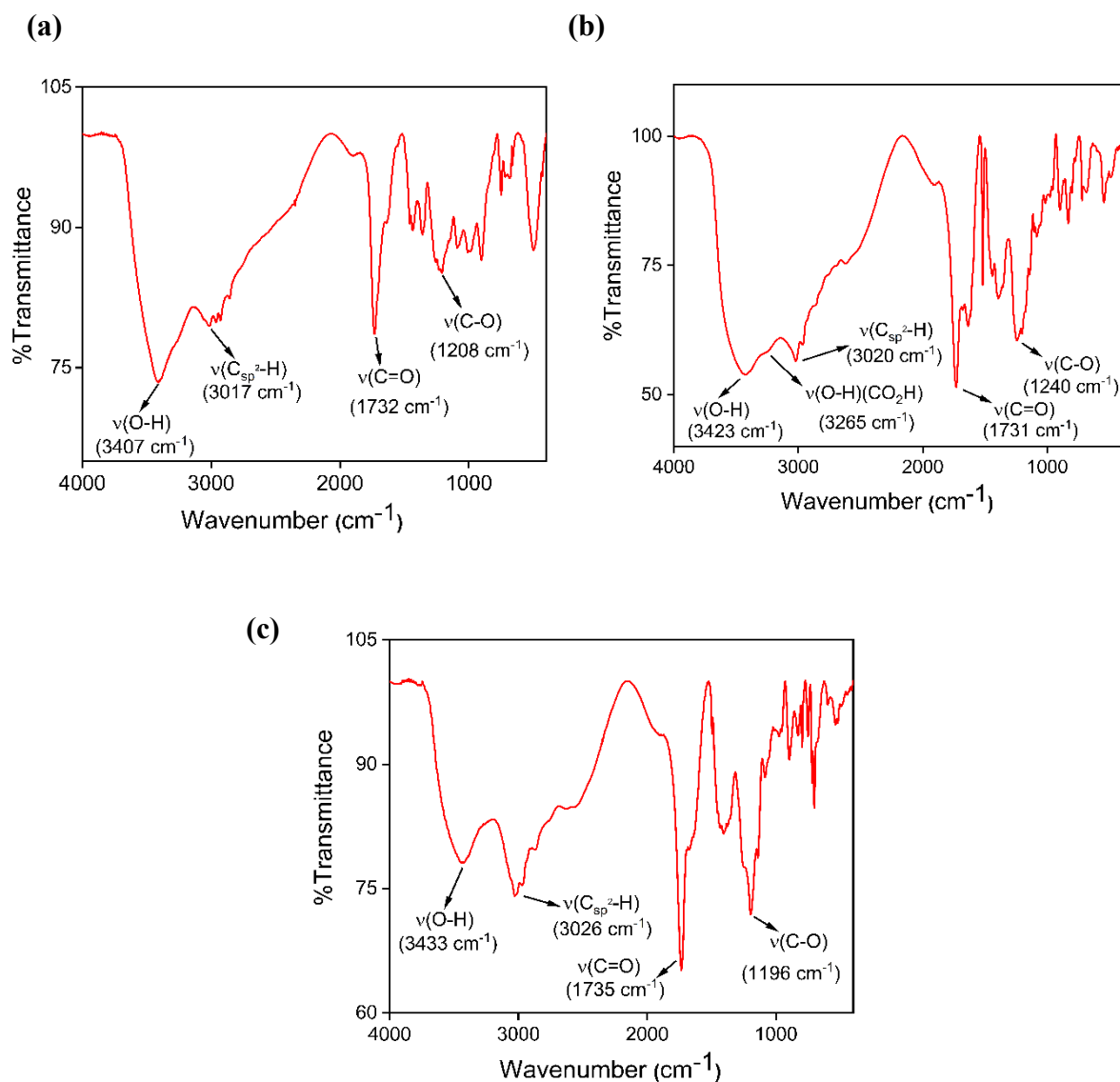


**Fig. S16** The solid-state FT-IR spectrum of (a)  $L^{trp}$ , (b)  $L^{tyr}$ , and (c)  $L^{phe}$  recorded in KBr pallet. Stretching frequencies ( $\nu/cm^{-1}$ ) of carbonyl functional group (C=O) in carboxylic moiety, aromatic ( $sp^2$ ) C-H and O-H groups are labelled.

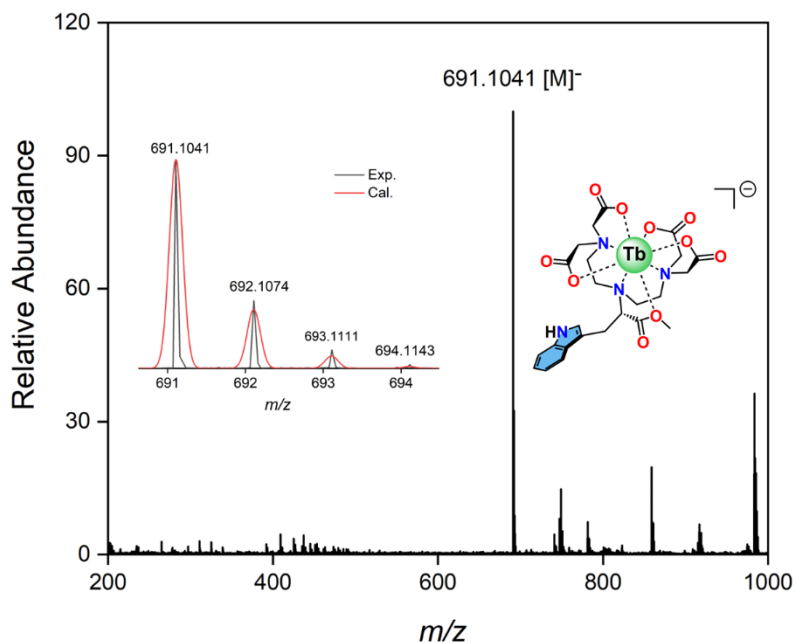


**Fig. S17** ESI-MS (-) spectra (full-range) of [Tb-L<sup>trp</sup>] in H<sub>2</sub>O and overlay of experimental isotopic distribution profile with theoretically calculated *m/z* values (inset). *m/z* for [M]<sup>-</sup>: exp.: 691.1041, calcd.: 691.1059.

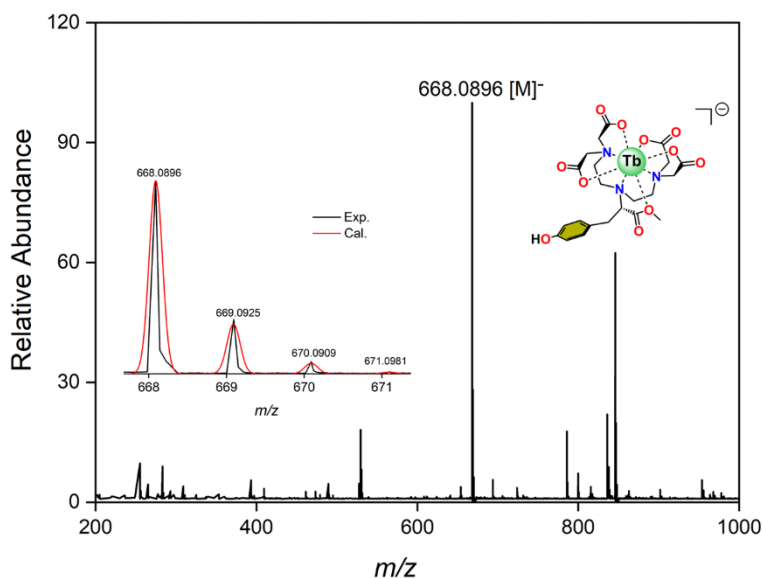


**Fig. S18** ESI-MS (-) spectra (full-range) of [Tb-L<sup>tyr</sup>] in H<sub>2</sub>O and overlay of experimental isotopic distribution profile with theoretically calculated *m/z* values (inset). *m/z* for [M]<sup>-</sup>: exp.: 668.0896, calcd.: 668.0899.

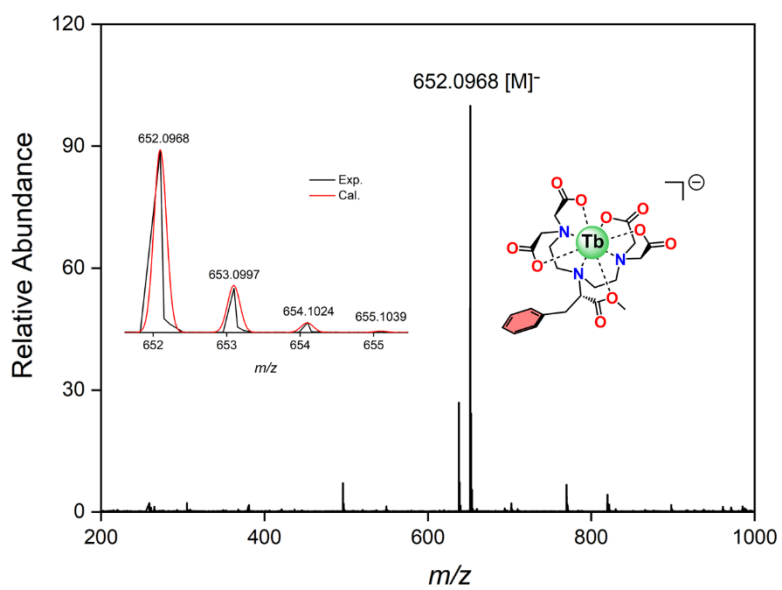


**Fig. S19** ESI-MS (-) spectra (full-range) of [Tb-L<sup>phe</sup>] in H<sub>2</sub>O and overlay of experimental isotopic distribution profile with theoretically calculated *m/z* values (inset). *m/z* for [M]<sup>-</sup>: exp.: 652.0968, calcd.: 652.0950.

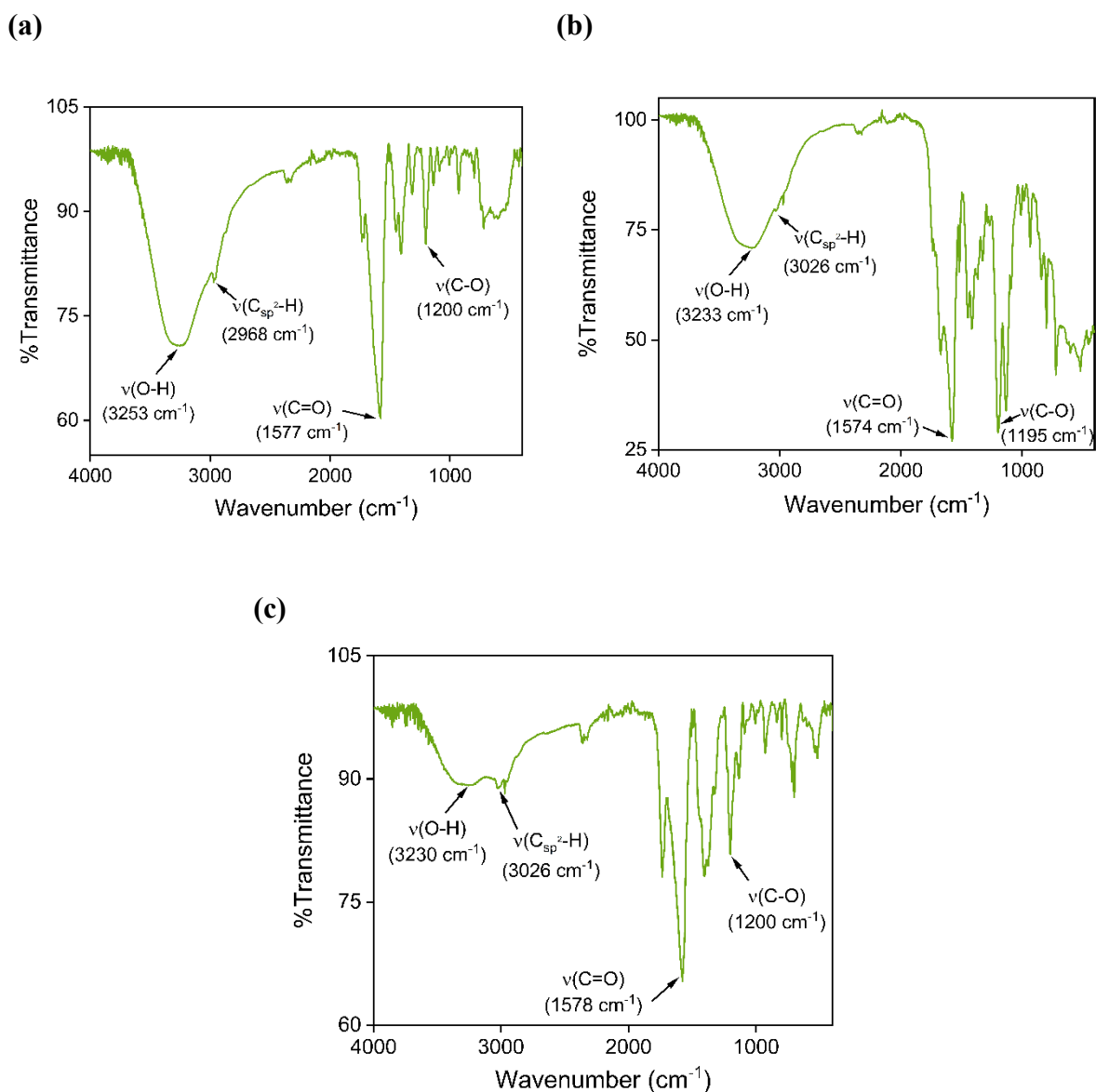


**Fig. S20** The solid-state FT-IR spectrum of (a) **[Tb-L<sup>trp</sup>]**, (b) **[Tb-L<sup>tyr</sup>]**, and (c) **[Tb-L<sup>phe</sup>]** recorded in KBr pellet. Stretching frequencies ( $\nu/\text{cm}^{-1}$ ) of carbonyl functional (C=O) group in carboxylic moiety, aromatic ( $\text{sp}^2$ ) C-H and O-H group are labeled.

## Spectroscopic studies:

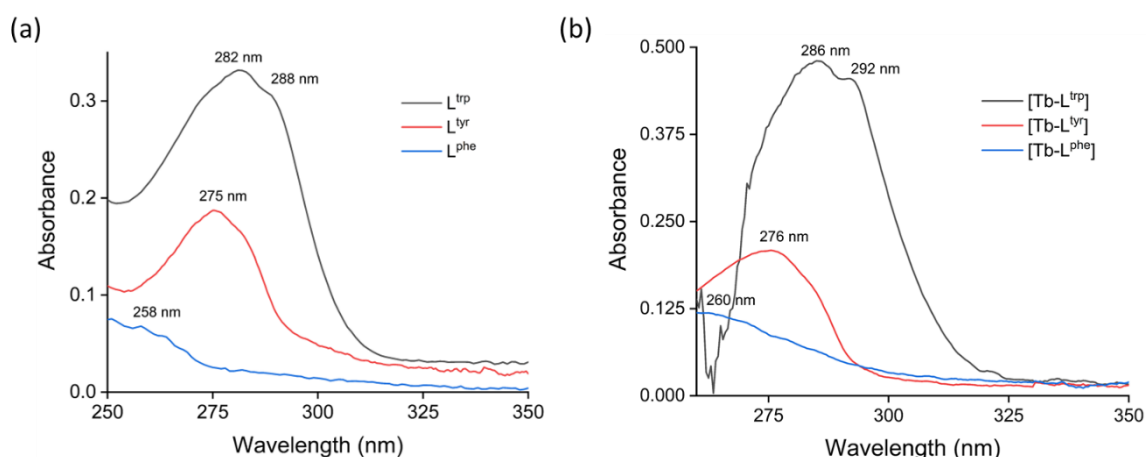


**Fig. S21** UV-Vis absorption spectrum of (a)  $L^{aa}$  ligands. For  $L^{trp}$ :  $\lambda_{max} = 282$  nm with a shoulder peak at 288 nm (*black*),  $L^{tyr}$ :  $\lambda_{max} = 275$  nm (*red*), and  $L^{phe}$ :  $\lambda_{max} = 258$  nm (*blue*). Conditions: 74  $\mu$ M of  $L^{aa}$  in 10 mM HEPES buffer (pH 7.2),  $T = 298$  K. (b)  $[Tb-L^{aa}]$  complexes. For  $[Tb-L^{trp}]$ :  $\lambda_{max} = 286$  nm with a shoulder peak at 292 nm (*black*),  $[Tb-L^{tyr}]$ :  $\lambda_{max} = 276$  nm (*red*), and  $[Tb-L^{phe}]$ :  $\lambda_{max} = 260$  nm (*blue*). Conditions: 0.16 mM of  $[Tb-L^{aa}]$  in 10 mM HEPES buffer (pH 7.2),  $T = 298$  K.

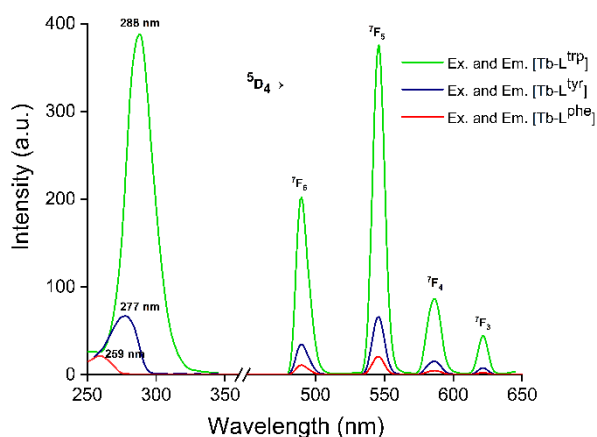


**Fig. S22** Excitation and time-resolved luminescence (TRL) spectra of  $[Tb-L^{aa}]$  complexes in HEPES buffer.  $[Tb-L^{trp}]$ :  $\lambda_{ex} = 288$  nm (*green*),  $[Tb-L^{tyr}]$ :  $\lambda_{ex} = 277$  nm (*blue*),  $[Tb-L^{phe}]$ :  $\lambda_{ex} = 259$  nm (*red*). Different spectral lines for Tb(III) centered emission spectra due to transition from  $^5D_4 \rightarrow ^7F_J$  energy states. Conditions: 25  $\mu$ M of  $[Tb-L^{aa}]$  in 10 mM HEPES buffer (pH 7.2), ex./em. slit width = 5 nm, delay and gate time = 0.5 ms,  $T = 298$  K.

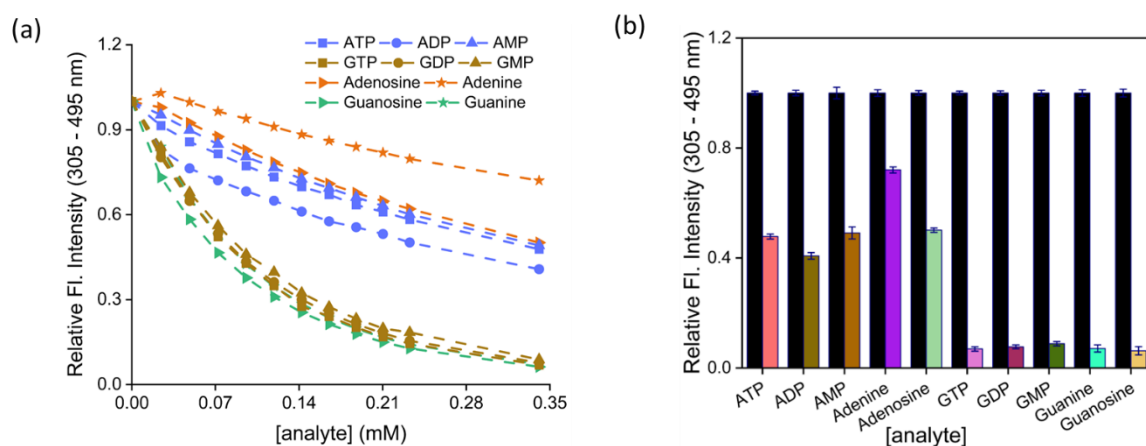


**Fig. S23** The relative changes in fluorescence intensity in  $L^{trp}$  (Integrated area from 305 nm to 495 nm) (a) as a function of the concentration of NPPs (0 – 0.34 mM). (b) The bar plot showing the changes in relative fluorescence intensity for free  $L^{trp}$  (*black*) with addition of different nucleobases, nucleosides and nucleotides (0.34 mM). Conditions:  $[L^{trp}] = 25 \mu\text{M}$  in 10 mM HEPES buffer (pH 7.2),  $\lambda_{ex} = 281 \text{ nm}$ , ex./em. slit width = 5 nm,  $T = 298 \text{ K}$ .

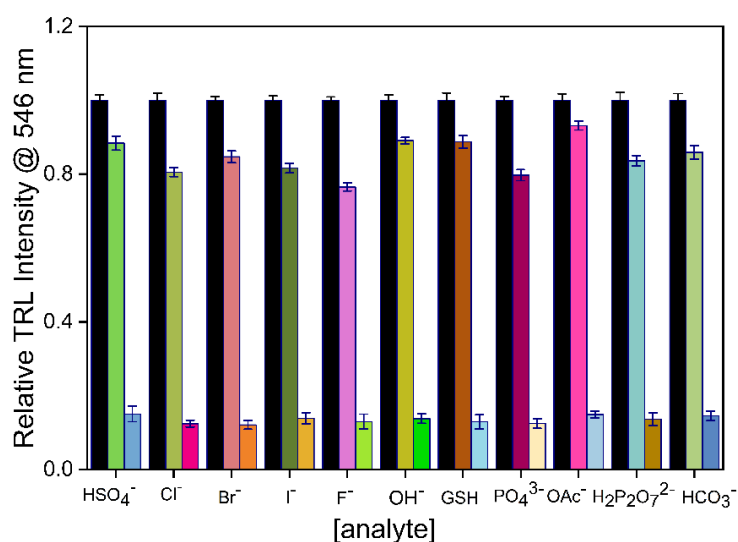


**Fig. S24** Relative changes of  ${}^5D_4 \rightarrow {}^7F_5$  emission peak intensity at 546 nm of  $[\text{Tb-L}^{trp}]$  in the absence of any analyte (*black*), followed by the addition of different interferents (0.64 mM) showing the negligible changes in emission intensity. The addition of GMP (0.64 mM) in every different set of mixtures results in a significant quenching in TRL-intensity, showcasing the selectivity towards G-NPPs. Conditions:  $[\text{Tb-L}^{trp}] = 25 \mu\text{M}$  in 10 mM HEPES buffer (pH 7.2),  $\lambda_{ex} = 290 \text{ nm}$ , ex./em. slit width = 5 nm, delay and gate time = 0.5 ms,  $T = 298 \text{ K}$ .

**Table S1.** Luminescence lifetime values of [Tb-L<sup>trp</sup>] in H<sub>2</sub>O/D<sub>2</sub>O and calculated  $q$  values, in the absence and presence of 30 eq. purine nucleotides. Condition: [Tb-L<sup>trp</sup>] = 25 μM in H<sub>2</sub>O and D<sub>2</sub>O, λ<sub>ex</sub> = 290 nm, ex./em. slit width = 5 nm, delay and gate time = 0.5 ms, T = 298 K.

Complex + NPPs (30 eq.)	τ <sub>H2O</sub> (ms)	τ <sub>D2O</sub> (ms)	$q$
[Tb-L <sup>trp</sup> ]	1.684	3.229	1.12
[Tb-L <sup>trp</sup> ] + GTP	1.767	3.072	0.902
[Tb-L <sup>trp</sup> ] + GDP	1.817	3.033	0.803
[Tb-L <sup>trp</sup> ] + GMP	1.838	3.173	0.844
[Tb-L <sup>trp</sup> ] + ATP	1.862	3.162	0.804
[Tb-L <sup>trp</sup> ] + ADP	1.877	3.123	0.762
[Tb-L <sup>trp</sup> ] + AMP	1.842	3.277	0.888

**Lifetime calculation:**

From equation 2, we can calculate the  $q$  values as follows:-

Initially, without addition of nucleotides,  $q$  value of [Tb-L<sup>trp</sup>] is,

$$q (\text{Tb}) = 5.0 \left( \frac{1}{1.684} - \frac{1}{3.229} - 0.06 \right) = 5.0 (0.594 - 0.31 - 0.06) = 5.0 \times 0.224 = 1.12$$

Similarly, after the addition of 30 eq. of GTP,  $q$  value of [Tb-L<sup>trp</sup>] is,

$$q (\text{Tb}) = 5.0 \left( \frac{1}{1.767} - \frac{1}{3.072} - 0.06 \right) = 5.0 (0.566 - 0.326 - 0.06) = 5.0 \times 0.18 = 0.9$$

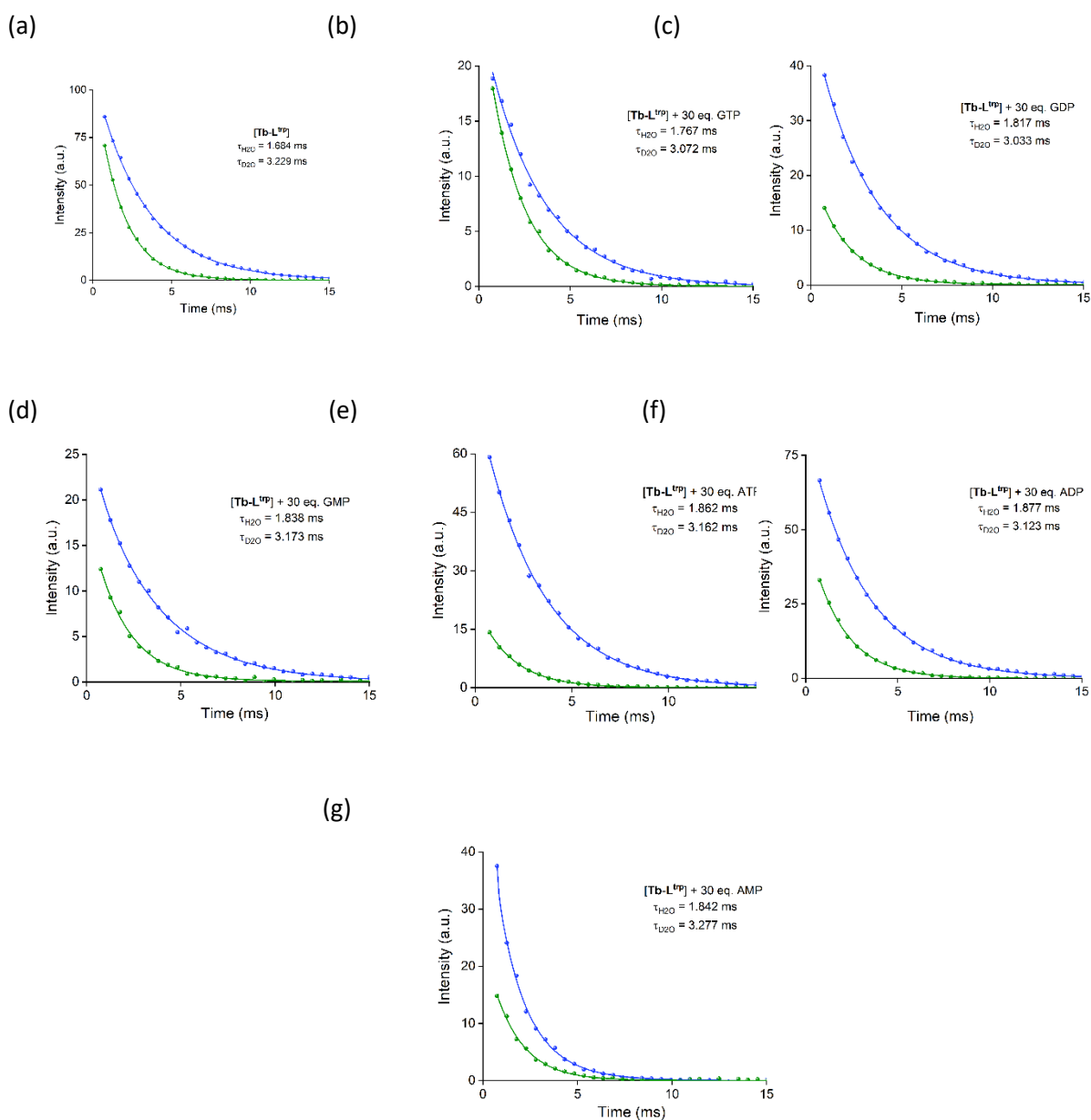


**Fig. S25** Luminescence lifetime of **[Tb-L<sup>trp</sup>]** in H<sub>2</sub>O (green) and D<sub>2</sub>O (blue), in the absence and presence of 30 eq. purine nucleotides. Condition: **[Tb-L<sup>trp</sup>]** = 25  $\mu\text{M}$  in H<sub>2</sub>O and D<sub>2</sub>O,  $\lambda_{\text{ex}} = 290 \text{ nm}$ , ex./em. slit width = 5 nm, delay and gate time = 0.5 ms, T = 298 K.

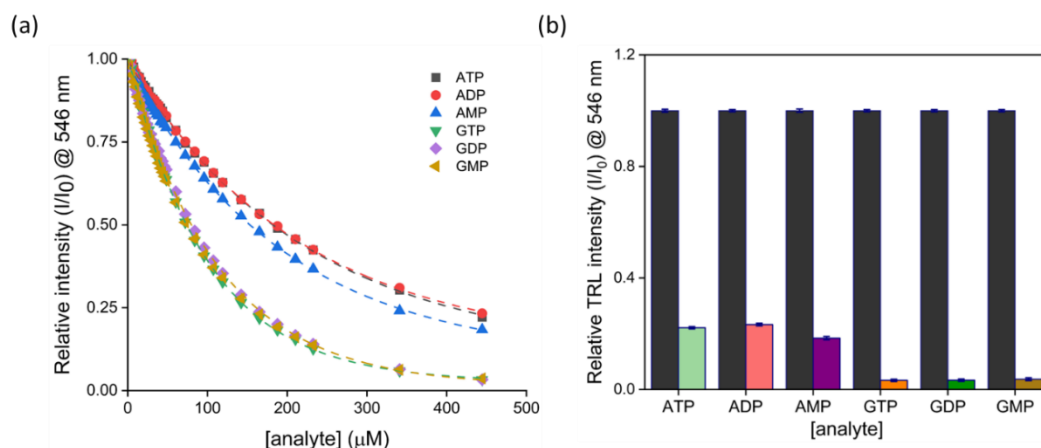


**Fig. S26** Time-resolved luminescence spectrum of  $[\text{Tb-L}^{\text{tyr}}]$ . Relative changes of  ${}^5\text{D}_4 \rightarrow {}^7\text{F}_5$  emission peak intensity ( $I/I_0$ ) at 546 nm (a) as a function of the concentration of NPPs (0 – 0.444 mM). (b) bar diagram showing the TRL-intensity of  $[\text{Tb-L}^{\text{tyr}}]$  in the free form (*black*) and with the addition of different NPPs (0.444 mM). Conditions: of  $[\text{Tb-L}^{\text{tyr}}] = 25 \mu\text{M}$  in 10 mM HEPES buffer (pH 7.2),  $\lambda_{\text{ex}} = 278 \text{ nm}$ , ex./em. slit width = 5 nm, delay and gate time = 0.5 ms,  $T = 298 \text{ K}$ .

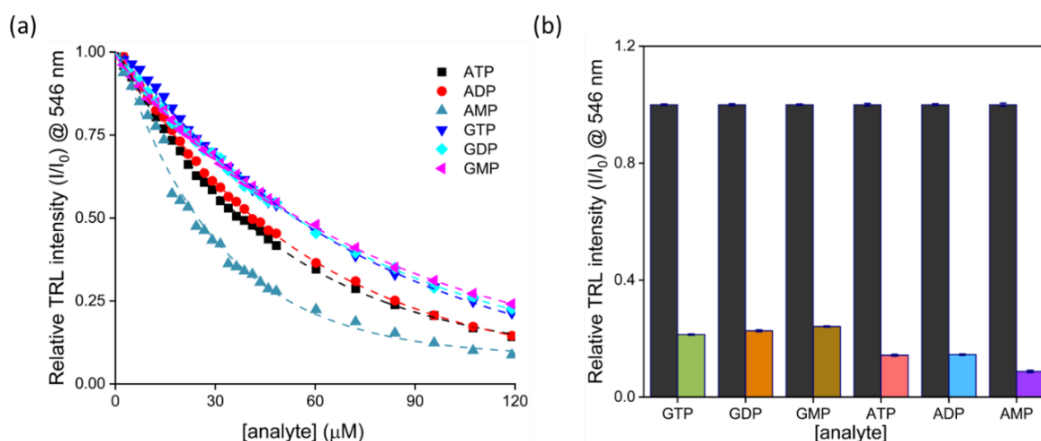


**Fig. S27** Time-resolved luminescence spectrum of  $[\text{Tb-L}^{\text{phe}}]$ . Relative changes of  ${}^5\text{D}_4 \rightarrow {}^7\text{F}_5$  emission peak intensity ( $I/I_0$ ) at 546 nm (a) as a function of the concentration of NPPs (0 – 0.119 mM). (b) bar diagram showing the TRL-intensity of  $[\text{Tb-L}^{\text{phe}}]$  in the free form (*black*) and with the addition of different NPPs (0.119 mM). Conditions:  $[\text{Tb-L}^{\text{phe}}] = 25 \mu\text{M}$  in 10 mM HEPES buffer (pH 7.2),  $\lambda_{\text{ex}} = 260 \text{ nm}$ , ex./em. slit width = 5 nm, delay and gate time = 0.5 ms,  $T = 298 \text{ K}$ .

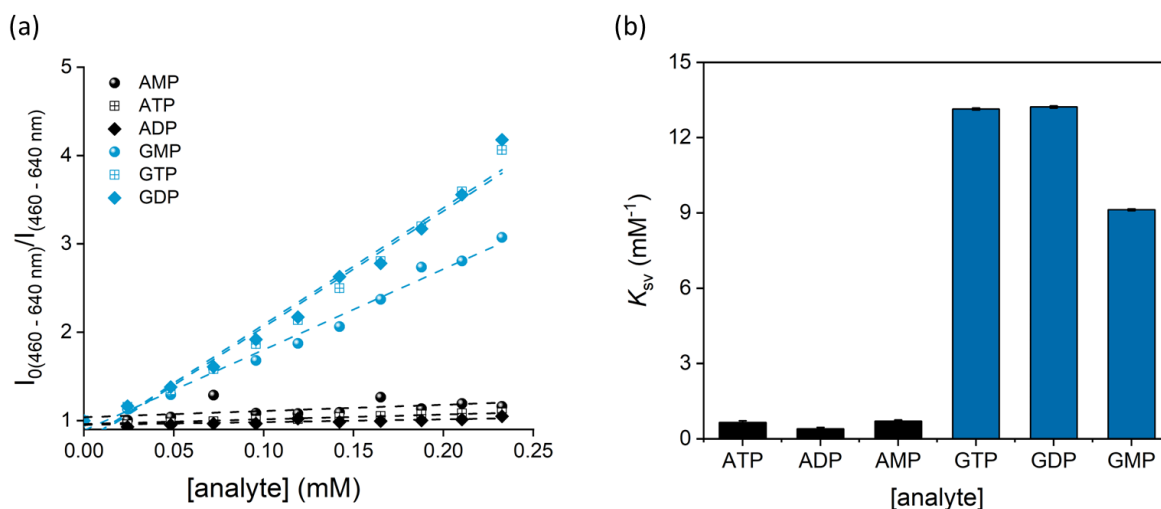


**Fig. S28** (a) Stern -Volmer plots from the TRL titration of  $[\text{Tb-L}^{\text{trp}}]$  with various nucleotides (0 – 0.23 mM). (b) Bar diagram showing the Stern-Volmer quenching constant ( $K_{\text{SV}}$ ) of  $[\text{Tb-L}^{\text{trp}}]$  with six nucleotides showing significantly higher  $K_{\text{SV}}$  for G-NPPs over A-NPPs. The TRL-intensity was calculated from the full range spectrum (460 – 640 nm). Conditions:  $[\text{Tb-L}^{\text{trp}}] = 25 \mu\text{M}$  in 10 mM HEPES buffer (pH 7.2),  $\lambda_{\text{ex}} = 290 \text{ nm}$ , ex./em. slit width = 5 nm, delay and gate time = 0.5 ms,  $T = 298 \text{ K}$ .

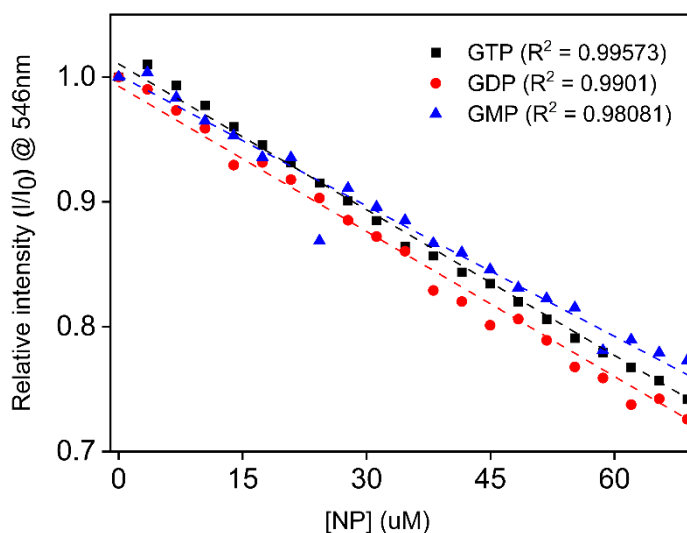


**Fig. S29** Plot for calculation of limit of detection (LOD) for G-NPPs using TRL titration data from  $[\text{Tb-L}^{\text{trp}}]$  ( $\lambda_{\text{max}} = 546 \text{ nm}$ ,  $\Delta J = 1$ ). Conditions:  $[\text{Tb-L}^{\text{trp}}] = 25 \mu\text{M}$  in 10 mM HEPES buffer (pH 7.2),  $\lambda_{\text{ex}} = 290 \text{ nm}$ , ex./em. slit width = 5 nm, delay and gate time = 0.5 ms,  $T = 298 \text{ K}$ .

**Table S2.** Calculation of LOD for G-NPPs using TRL-titration data from [Tb-L<sup>trp</sup>] ( $\lambda_{\max}$  = 546 nm,  $\Delta J = 1$ ). Conditions: [Tb-L<sup>trp</sup>] = 25  $\mu$ M in 10 mM HEPES buffer (pH 7.2),  $\lambda_{\text{ex}}$  = 290 nm, ex./em. slit width = 5 nm, delay and gate time = 0.5 ms,  $T = 298$  K.

Nucleotides (G-NPPs)	Slope (S)	R <sup>2</sup>	Standard error ( $\sigma$ )	LOD = 3.3*( $\sigma/S$ ) (ppm)
GTP	-0.00389	0.99573	0.00258	1.13
GDP	-0.00387	0.9901	0.00393	1.47
GMP	-0.00348	0.98081	0.00494	1.69

### References

1. Y. Azuma, M. Imanishi, T. Yoshimura, T. Kawabata and S. Futaki, *Angew. Chem. Int. Ed.*, 2009, **48**, 6853-6856.
2. Anelli, Pier Lucio; Lolli, Marco; Fedeli, Franco; Virtuani, Mario, World Intellectual Property Organization, WO9805626, 1998.